

Amplitude squeezing in a pump-noise-suppressed laser oscillator

Y. Yamamoto and S. Machida

Electrical Communication Laboratories, Nippon Telegraph and Telephone Corporation, Musashinoshi, Tokyo 180, Japan

O. Nilsson

The Royal Institute of Technology, Stockholm, S-10014, Sweden

(Received 9 April 1986)

This paper clarifies the origins of the standard quantum limit for the amplitude noise of a laser-oscillator outgoing field. The amplitude noise within the cavity bandwidth, $\Omega \leq \omega/Q$, is ultimately caused by the pump amplitude fluctuation, while that above the cavity bandwidth, $\Omega \geq \omega/Q$, is due to the field zero-point fluctuation. The uncertainty product of the amplitude- and phase-noise spectra at an extremely high pumping level is still larger than the Heisenberg minimum-uncertainty product because of the presence of nonstationary phase-diffusion noise. In this sense, an ordinary laser oscillator is not a quantum-limited device. This paper suggests that a laser oscillator can produce an amplitude-squeezed state in itself if the pump amplitude fluctuation is suppressed below the ordinary shot-noise level. The paper discusses possible schemes for suppressing pump fluctuation, commutator bracket preservation without pump fluctuation, and resulting amplitude and phase spectra. The similarity of and difference between a pump-noise-suppressed laser and a cavity degenerate parametric amplifier are delineated.

I. INTRODUCTION

A squeezed state of light features reduced quantum noise in one quadrature component below the standard quantum limit $\langle \Delta \hat{a}_i^2 \rangle < \frac{1}{4}$ ($i=1$ or 2).¹⁻³ The minimum-uncertainty product, $\langle \Delta \hat{a}_1^2 \rangle \langle \Delta \hat{a}_2^2 \rangle = \frac{1}{16}$, can still be preserved by the enhanced quantum noise in another quadrature component. When the quantum noise is finally reduced to zero as shown in Fig. 1(a), the mean photon number goes to infinity. This trade-off relation between quantum-noise reduction and required mean photon number places the limit on the signal-to-noise ratio

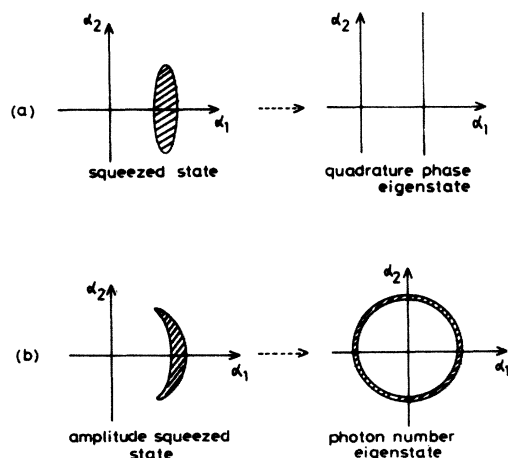


FIG. 1. Quasiprobability density $\langle \alpha | \rho | \alpha \rangle$ of a squeezing state and an amplitude-squeezed state (or number-phase minimum-uncertainty state). ρ is the density operator and $|\alpha\rangle$ is a coherent state. $\alpha_1 = \text{Re}(\alpha)$ and $\alpha_2 = \text{Im}(\alpha)$. A quadrature-phase eigenstate and a photon-number eigenstate are the ultimate cases for these two states.

improvement for a fixed mean photon number.

A squeezed state can be generated by unitary evolution from a coherent state. The current experimental efforts to generate a squeezed state of light employ a variety of nonlinear optical processes.⁴⁻⁶ Recently, Slusher *et al.* observed squeezing in a cavity four-wave-mixing scheme.⁷

In addition, the present authors proposed a generation scheme for another kind of nonclassical photon state, the "amplitude-squeezed state" or "number-phase minimum-uncertainty state."⁸⁻¹² An amplitude-squeezed state features reduced amplitude (or photon-number) noise below the standard quantum limit, $\langle \Delta \hat{n}^2 \rangle < \langle \hat{n} \rangle$. The minimum-uncertainty product between the photon number and phase, $\langle \Delta \hat{n}^2 \rangle \langle \Delta \hat{\phi}^2 \rangle = \frac{1}{4}$, can still be preserved by the enhanced phase noise, $\langle \Delta \hat{\phi}^2 \rangle > 1/4 \langle \hat{n} \rangle$. The unique feature of an amplitude-squeezed state is that the photon-number noise can be finally reduced to zero (photon-number eigenstate) as shown in Fig. 1(b) without requiring an infinite mean photon number.

It is known that an amplitude-squeezed state can be generated by unitary evolution from a coherent state, but the nonunitary processes such as a measurement process or a dissipative system can be also involved to generate it. One generation scheme is based on the quantum non-demolition measurement of the photon number using an optical Kerr medium¹¹ and the (linear) negative feedback.⁹ Sub-Poissonian photoelectron statistics were actually observed in a negative-feedback laser using a destructive photon detector.¹⁰ A sub-Poissonian light generation scheme based on a similar principle has been recently discussed,^{13,14} but the light produced by this scheme is weak and incoherent.

The photon-number eigenstate provides the maximum channel capacity in optical communication,^{15,16} and its information can be read out repeatedly without disturbing

the state, that is, without absorbing the photons by the quantum nondemolition measurement.¹¹ The photon-number eigenstate is also useful for improving optical interferometer performance.¹⁷ It has been theoretically predicted that a noiseless photon amplifier exists which transforms $|n\rangle \rightarrow |Gn\rangle$.¹⁸ All of these features suggest a tremendous performance gain over an ordinary coherent-state and squeezed-state system obtainable by means of the photon-number eigenstate.

In this paper a new scheme is proposed for generating an amplitude-squeezed state. We will show that a laser oscillator can produce an amplitude-squeezed state provided that pump amplitude fluctuation can be suppressed below the ordinary shot-noise level.¹⁹

In Secs. II and III, we focus our discussion specifically on why a laser generates a coherent state instead of an amplitude-squeezed state, even though its amplitude-stabilizing force induced by gain saturation is increased with a pumping level.

We briefly review the quantum-mechanical theory of a laser from such viewpoints. What we find is that there is a subtle balance between the cooperative force induced by gain saturation and the fluctuating force imposed by the heat baths through the fluctuation-dissipation theorem. Such a balance between the cooperative force and the fluctuating force establishes the standard quantum-limited (or shot-noise-limited) photon flux. The origin of this amplitude noise is the pump amplitude fluctuation (not pump phase fluctuation) within the cavity bandwidth, $\Omega \leq \omega/Q$, and is the field zero-point fluctuation above the cavity bandwidth, $\Omega \geq \omega/Q$.

From the observations made in Secs. II and III, two interesting possibilities for obtaining an amplitude-squeezed state directly from a laser oscillator are suggested. One possibility is breaking the balance between the two forces by artificially enhancing the cooperative force (gain saturation). A laser oscillator incorporating a quantum nondemolition detector and a linear feedback loop⁸⁻¹² specifically realizes this possibility. The other possibility is breaking the balance by suppressing pump fluctuation, which is the express subject of this paper.

In Sect. IV, we briefly discuss a possible scheme for suppressing this pump fluctuation below the usual shot-noise limit.²⁰

In Sec. V we demonstrate that the absence of pump fluctuation does not contradict quantum-mechanical consistency, even though the shot-noise-limited pump fluctuation has been widely accepted in the conventional quantum-mechanical laser theory.²¹⁻²³ It is shown that the commutator bracket for the cavity internal field and the output field are properly preserved without pump fluctuation.

We calculate the amplitude and phase spectra in Sec. VI for a pump-noise-suppressed laser oscillator and compare them with those of a cavity degenerate parametric amplifier. The photon statistics for the cavity internal field is sub-Poissonian. The variance of the photon number takes the minimum value of $\frac{1}{2}\langle \hat{n} \rangle$ at an extremely high pumping level. That is, the amplitude-squeezing factor is only one-half for the internal field. The photon flux spectrum emerging out of the cavity is, on the other hand, decreased

below the standard quantum limit by the factor $\Omega^2/(\omega/Q)^2$ within the cavity bandwidth. So the infinite amplitude squeezing is obtained in the low-frequency limit, $\Omega \ll \omega/Q$.

Finally, in Sec. VII, we confirm the results presented in this paper from the discussion based on particle-number preservation.

II. OPERATOR LANGEVIN EQUATIONS

To adequately ascertain why a laser generates a coherent state instead of an amplitude-squeezed state, we will here briefly review the quantum-mechanical laser theory based on the operator Langevin equations. Although a conventional theory treats only the noise properties of the cavity internal field, it has recently been shown both for a laser²⁴ and for a degenerate parametric amplifier²⁵ that the external- and internal-field fluctuations differ. This difference stems from the fact that the transmitted internal field and the reflected field zero-point fluctuation are quantum-mechanically correlated and interfere with each other as shown in Fig. 2.

The quantum-mechanical Langevin equation for the cavity internal-field operator \hat{A} is given by

$$\frac{d}{dt}\hat{A} = \frac{1}{2} \left[\frac{\omega}{Q} + 2j(\omega - \omega_0) - \frac{\omega}{\mu^2}(\tilde{\chi}_i - j\tilde{\chi}_r) \right] \hat{A} + \tilde{G} + \hat{g} + \hat{f}. \quad (2.1)$$

Here ω/Q is the photon decay rate, which is decomposed into the internal loss contribution ω/Q_0 and the output coupling contribution ω/Q_e as

$$\frac{\omega}{Q} = \frac{\omega}{Q_0} + \frac{\omega}{Q_e}. \quad (2.2)$$

ω_0 and ω are the empty cavity resonance frequency and the actual oscillation frequency. μ is a nonresonant refractive index. $\tilde{\chi} = \tilde{\chi}_r + j\tilde{\chi}_i$ is the complex susceptibility operator. The real part $\tilde{\chi}_r$ represents an anomalous index dispersion, and the imaginary part $\tilde{\chi}_i$ indicates the stimulated emission gain

$$\frac{\omega}{\mu^2}\tilde{\chi}_i = \tilde{E}_{cv} - \tilde{E}_{vc}. \quad (2.3)$$

Here the subscripts c and v indicate the conduction and valence electrons. Although the detailed expressions for the stimulated emission rate \tilde{E}_{cv} and absorption rate \tilde{E}_{vc} depend on the actual laser systems, they are not necessary for our purpose here. The operators $\tilde{\chi}_r$ and $\tilde{\chi}_i$ are already averaged for heat baths, but still depend on such system operators as the population-difference operator.

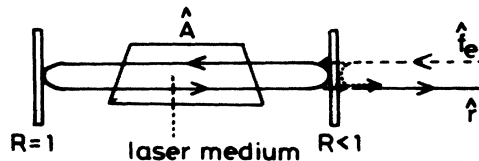


FIG. 2. Theoretical model for a laser oscillator.

\tilde{G} , \hat{g} , and \hat{f} are fluctuating noise operators, which represent the coupling of the field \hat{A} to heat baths. The noise operator \tilde{G} originates from the Fermi commutation relation for the electron operator \tilde{b} .²¹ This noise operator enters into the field Langevin equation (2.1) through the adiabatic elimination of the dipole-moment operator. The noise operators \hat{g} and \hat{f} preserve the boson commutation relation for the photon operator \hat{A} ,

$$[\hat{A}, \hat{A}^\dagger] = 1, \quad (2.4)$$

for its dissipation process, that is, its coupling process to the heat baths (internal loss and mirrors).

The correlation functions for these noise operators can be determined from these requirements mentioned above (fluctuation-dissipation theorem). When the heat baths exhibit broad frequency spectra and therefore enable the dissipation processes to be considered as Markovian, the correlation functions of the two Hermitian (real and imaginary parts) operators for each noise operator are²¹⁻²³

$$\begin{aligned} \langle \tilde{G}_r(t) \tilde{G}_r(u) \rangle &= \langle \tilde{G}_i(t) \tilde{G}_i(u) \rangle \\ &= \delta(t-u) \frac{1}{4} (\langle \tilde{E}_{cv} \rangle + \langle \tilde{E}_{vc} \rangle), \end{aligned} \quad (2.5)$$

$$\langle \hat{g}_r(t) \hat{g}_r(u) \rangle = \langle \hat{g}_i(t) \hat{g}_i(u) \rangle = \delta(t-u) \frac{\omega}{4Q_0}, \quad (2.6)$$

and

$$\langle \hat{f}_r(t) \hat{f}_r(u) \rangle = \langle \hat{f}_i(t) \hat{f}_i(u) \rangle = \delta(t-u) \frac{\omega}{4Q_e}. \quad (2.7)$$

Here \tilde{G}_r and \tilde{G}_i are defined by

$$\tilde{G}_r = \frac{1}{2} (\tilde{G} + \tilde{G}^\dagger),$$

and

$$\tilde{G}_i = \frac{1}{2j} (\tilde{G} - \tilde{G}^\dagger).$$

\hat{f}_r , \hat{f}_i , \hat{g}_r , and \hat{g}_i are defined by similar equations. In this case, we use a caret and a tilde to denote operators for the photon field and the electron systems, respectively.

The noise operator \hat{f} represents the contribution made by the zero-point fluctuation \hat{f}_e , coupled into the cavity through the partially reflecting mirror as shown in Fig. 2. If the incident field (not necessarily the zero-point fluctuation) is normalized such that $\langle \hat{f}_e^\dagger \hat{f}_e \rangle$ represents the average photon flux (number per second), \hat{f} in (2.1) is related to \hat{f}_e by²⁶

$$\hat{f} = (\omega/Q_e)^{1/2} \hat{f}_e. \quad (2.8)$$

The conventional quantum-mechanical laser theory^{21,23} does not necessarily mention this origin of the noise operator \hat{f} because in the conventional theory the internal field is the only "system" of interest, while the external field outside of the cavity is considered to be one of the "heat baths." Since we are interested in the external field, it must also be treated as another system.

As shown in Fig. 2, the external output field \hat{r} consists of the transmitted internal field and the reflected part of the incident zero-point fluctuation as

$$\hat{r} = \hat{f}_e + (\omega/Q_e)^{1/2} \hat{A}. \quad (2.9)$$

This relation is obtained from the argument based on time reversal,²⁶ or from the direct analysis of waves bouncing back and forth in a Fabry-Perot resonator.²⁴

The electron system can be described by one equation of motion for a total population difference operator

$$\tilde{N}_c = \sum_k (\tilde{b}_{2k}^\dagger \tilde{b}_{2k} - \tilde{b}_{1k}^\dagger \tilde{b}_{1k}),$$

when the active medium is a homogeneously broadening one. The summation is over all upper- and lower-level electronic states denoted by the wave number k .

The operator Langevin equation for \tilde{N}_c after the adiabatic elimination of the dipole-moment operator is given as^{21,23}

$$\frac{d}{dt} \tilde{N}_c = p - \frac{\tilde{N}_c}{\tau_{sp}} - (\tilde{E}_{cv} - \tilde{E}_{vc}) \hat{n} - \tilde{E}_{cv} + \tilde{\Gamma}_p + \tilde{\Gamma}_{sp} + \tilde{\Gamma}. \quad (2.10)$$

Here p and $1/\tau_{sp}$ are the pump rate and the spontaneous population-inversion decay rate. The fluctuating noise operators for these two processes are denoted by $\tilde{\Gamma}_p$ and $\tilde{\Gamma}_{sp}$. Finally, $\hat{n} = \hat{A}^\dagger \hat{A}$ is a photon-number operator.

The spontaneous population-inversion decay process is a stimulated emission process induced by the (field) zero-point fluctuations of all continuous modes in an active medium except for the lasing mode. The spontaneous decay induced by the zero-point fluctuation of the lasing mode is represented by the fourth term, \tilde{E}_{cv} , of (2.10). Since these zero-point fluctuations have only a very short memory, and the decay process is considered to be Markovian, the correlation function for $\tilde{\Gamma}_{sp}$ is given by^{21,23}

$$\langle \tilde{\Gamma}_{sp}(t) \tilde{\Gamma}_{sp}(u) \rangle = \delta(t-u) \frac{\langle \tilde{N}_c \rangle}{\tau_{sp}}. \quad (2.11)$$

The shot-noise character of (2.11) stems directly from the shot-noise character of the zero-point fluctuations.

In a conventional quantum-mechanical laser theory, the pumping process is treated as the reverse process of the spontaneous emission.²¹ This treatment implicitly assumes incoherent light pumping. As noted earlier, incoherent light has a broad spectrum of frequency and a very short memory time. The correlation function for $\tilde{\Gamma}_p$ is then given by^{21,23}

$$\langle \tilde{\Gamma}_p(t) \tilde{\Gamma}_p(u) \rangle = \delta(t-u) p, \quad (2.12)$$

which holds even when the pump light is coherent laser radiation. This is because the pumping process, i.e., the photoelectron emission process is a self-exciting Poisson point process, as was mentioned earlier.

If the pump light is sub-Poissonian light or near-photon-number eigenstate light and the quantum efficiency of optical pumping is close to unity, the photoelectron-emission process becomes regulated and exhibits smaller pump noise than the ordinary shot-noise-limited pump noise (2.12). The phase noise of the pump light does not contribute to the output field noise of a laser oscillator at all, because the pumping process is actu-

ally a photon-counting process. Therefore, the increased phase noise of the sub-Poissonian light or near-photon-number eigenstate light, as compared with a coherent state, does not affect the statistical properties of laser emission. This is a remarkable difference between a laser oscillator and a parametric oscillator, in which the phase noise of the pump wave directly affects the noise properties of parametric emission. In Sec. IV we will outline several effective schemes for suppressing the pump amplitude fluctuation below the ordinary shot-noise limit.

The noise operator $\tilde{\Gamma}$ originates from the dipole-moment fluctuating operator. This noise operator enters into the population-inversion Langevin equation through the adiabatic elimination of the dipole-moment operator. The correlation function for $\tilde{\Gamma}$ is

$$\langle \tilde{\Gamma}(t)\tilde{\Gamma}(u) \rangle = \delta(t-u) (\langle \tilde{E}_{cv} \rangle + \langle \tilde{E}_{vc} \rangle) \langle \hat{n} \rangle. \quad (2.13)$$

Since the two operators \tilde{G} and $\tilde{\Gamma}$ come from the same origin (the Langevin noise source for the dipole-moment operator), they have the correlation

$$\langle \tilde{G}_r(t)\tilde{\Gamma}(u) \rangle = -\delta(t-u) \frac{1}{2} (\langle \tilde{E}_{cv} \rangle + \langle \tilde{E}_{vc} \rangle) \langle \hat{A} \rangle, \quad (2.14)$$

and

$$\langle \tilde{G}_i(t)\tilde{\Gamma}(u) \rangle = 0. \quad (2.15)$$

III. ORIGINS FOR STANDARD QUANTUM LIMIT

A. Laser amplifier

If a laser oscillator is biased below its oscillation threshold and an external signal is injected into the cavity, the reflected wave from the cavity can be considered to be a linearly amplified output signal. The quantum noise of such a cavity laser amplifier was treated either by the operator Langevin equation or by the quantum-mechanical Fokker-Planck equation.²⁶ Here, we present a discussion on the origin for the standard quantum limit of a laser amplifier stemming from the dipole-moment fluctuation operator \tilde{G} .

The noise operator \hat{f} in (2.1) is not considered to be a zero-point fluctuation \hat{f}_e but rather to be an actual input-signal operator \hat{b}_e . If we assume that the input-signal frequency is exactly tuned to the active Fabry-Perot cavity resonant frequency, and that the internal loss is negligible, (2.1) can be rewritten as

$$\frac{d}{dt} \hat{A} = -\frac{1}{2} \left[\frac{\omega}{Q_e} - \tilde{E}_{cv} \right] \hat{A} + (\omega/Q_e)^{1/2} \hat{b}_e + \tilde{G}. \quad (3.1)$$

Here we assumed that the stimulated absorption \tilde{E}_{vc} is negligible, that is, that a laser amplifier features an ideal population inversion. The stimulated emission rate \tilde{E}_{cv} is already averaged for heat-bath coordinates, with their fluctuation terms imposed by heat baths being denoted by \tilde{G} . Although they are still dependent on the population-inversion operator \tilde{N}_c , the \tilde{E}_{cv} fluctuation is negligible for a linear laser amplifier, in which the population difference \tilde{N}_c is determined only by the pump rate p , the spontane-

ous decay rate $1/\tau_{sp}$, and their noise sources Γ_p and $\tilde{\Gamma}_{sp}$. The fluctuations of the photon field and of the population difference are decoupled in this operational region. Therefore, we can treat \tilde{E}_{cv} in (3.1) as the c -number stimulated emission rate $\langle \tilde{E}_{cv} \rangle$.

If the input signal has a bandwidth much narrower than the amplifier bandwidth $B = \omega/Q_e - \langle \tilde{E}_{cv} \rangle$, we can employ a single-mode description of the system. The input and output signal modes, \hat{b}_s and \hat{r}_s , which are defined by the bandwidth B_s of the input signal, or equivalently by the measurement time interval, $T_s = 1/B_s$, are related by

$$\begin{aligned} \hat{r}_s &= -\hat{b}_s + (\omega/Q_e)^{1/2} \hat{A}_s \\ &= \frac{\omega/Q_e + \langle \tilde{E}_{cv} \rangle}{\frac{\omega}{Q_e} - \langle \tilde{E}_{cv} \rangle} \hat{b}_s + \frac{2(\omega/Q_e)^{1/2}}{\frac{\omega}{Q_e} - \langle \tilde{E}_{cv} \rangle} \tilde{G}_s. \end{aligned} \quad (3.2)$$

Here the noise operator is also renormalized from \tilde{G} by the bandwidth B_s or the time interval T_s . When we assign

$$(G_e)^{1/2} = \frac{\frac{\omega}{Q_e} + \langle \tilde{E}_{cv} \rangle}{\frac{\omega}{Q_e} - \langle \tilde{E}_{cv} \rangle} > 1, \text{ and } \tilde{c}_s = \langle \tilde{E}_{cv} \rangle^{-1/2} \tilde{G}_s,$$

and use the relation, $\omega/Q_e \simeq \langle \tilde{E}_{cv} \rangle$ (high-gain amplifier), (3.2) can be rewritten as

$$\hat{r}_s = (G_e)^{1/2} \hat{b}_s + (G_e - 1)^{1/2} \tilde{c}_s. \quad (3.3)$$

Here, from (2.5), the noise operator \tilde{c}_s has the same commutator bracket as the single-mode zero-point fluctuation,

$$[\tilde{c}_s, \tilde{c}_s^\dagger] = 1. \quad (3.4)$$

Equation (3.3) can be derived for any linear amplifier in a more universal manner by imposing the boson commutator bracket preservation²⁷ $[\hat{b}_s, \hat{b}_s^\dagger] = [\hat{r}_s, \hat{r}_s^\dagger] = 1$. The above discussion delineates the noise source \tilde{c}_s which is required for the commutator bracket preservation, is in fact the dipole-moment fluctuation operator \tilde{G} for a laser amplifier. The origins of the noise source \tilde{c}_s are different for each amplifier system, and, for instance, are the field zero-point fluctuation at an idler frequency band for a parametric amplifier, or the phonon-mode fluctuation operator for a Raman and Brillouin amplifier.¹⁶ This noise source \tilde{c}_s imposes the standard quantum limit of a linear amplifier²⁷ on the simultaneous measurement of two conjugate observables.¹⁶

Although the pump noise does not affect the standard quantum limit of a laser amplifier, it will be made clear in Sec. III B that the pump noise supplants the role of the dipole-moment fluctuation operator in a highly saturated laser oscillator. The effect of the dipole-moment fluctuation operator is completely suppressed by the gain saturation as far as the amplitude noise is concerned.

B. Laser oscillator internal field

Let us focus here on the amplitude and phase noise of a laser oscillator pumped at well above the threshold. For

this region, the operator Langevin equations (2.1) and (2.10) can be solved by the quasilinearization procedure. The internal field operator \hat{A} and population inversion operator \tilde{N}_c are expressed as

$$\hat{A} = (A_0 + \Delta\hat{A}) \exp(-j\Delta\hat{\phi}), \quad (3.5a)$$

and

$$\tilde{N}_c = N_{c0} + \Delta\tilde{N}_c, \quad (3.5b)$$

where $\Delta\hat{A}$, $\Delta\hat{\phi}$, and $\Delta\tilde{N}_c$ are the Hermitian amplitude, phase, and population-inversion fluctuating operators, and A_0 and N_{c0} are the average field amplitude and population inversion (c numbers). Although a Hermitian phase operator does not exist in a strict quantum-mechanical sense, it is known that (3.5a) is still a reasonable approximation when the photon number A_0^2 is much larger than unity.²⁸

The power spectra of $\Delta\hat{A}$ and $\Delta\hat{\phi}$ are calculated by using (3.5a) and (3.5b) in (2.1) and (2.10) as (Appendix A)

$$P_{\Delta\hat{A}}(\Omega) = [A_3^2 \langle |\tilde{\Gamma}_p(\Omega)|^2 + |\tilde{\Gamma}_{sp}(\Omega)|^2 + |\tilde{\Gamma}(\Omega)|^2 \rangle + (\Omega^2 + A_1^2) \langle |\tilde{G}_r(\Omega)|^2 + |\hat{g}_r(\Omega)|^2 + |\hat{f}_r(\Omega)|^2 \rangle - 2A_1A_3 \langle \tilde{G}_r(\Omega)\tilde{\Gamma}(\Omega) \rangle] / [(\Omega^2 + A_2A_3)^2 + \Omega^2A_1^2], \quad (3.6)$$

and

$$P_{\Delta\hat{\phi}}(\Omega) = \frac{\langle |\tilde{G}_i(\Omega)|^2 + |\hat{g}_i(\Omega)|^2 + |\hat{f}_i(\Omega)|^2 \rangle}{\Omega^2A_0^2} + A_4^2 [\langle |\tilde{\Gamma}_p(\Omega)|^2 + |\tilde{\Gamma}_{sp}(\Omega)|^2 + |\tilde{\Gamma}(\Omega)|^2 \rangle + \left(\frac{A_2}{\Omega}\right)^2 \langle |\tilde{G}_r(\Omega)|^2 + |\hat{f}_r(\Omega)|^2 + |\hat{g}_r(\Omega)|^2 \rangle] \times [(\Omega^2 + A_2A_3)^2 + \Omega^2A_1^2]^{-1}. \quad (3.7)$$

Here the parameters A_1 – A_4 , are given by

$$A_1 = \left[\frac{1}{\tau_{sp}} + \frac{1}{\tau_{st}} \right] = \frac{1}{\tau_{sp}} (1 + n_{sp}R), \quad (3.8a)$$

$$A_2 = 2 \frac{\omega}{Q} A_0, \quad (3.8b)$$

$$A_3 = \frac{1}{2A_0\tau_{st}} = \frac{n_{sp}R}{2A_0\tau_{sp}}, \quad (3.8c)$$

and

$$A_4 = \frac{\alpha}{2A_0^2\tau_{st}} = \frac{\alpha n_{sp}R}{2A_0^2\tau_{sp}}. \quad (3.8d)$$

τ_{st} , n_{sp} , α , and R are the stimulated population-inversion decay rate, the population-inversion parameter, the detuning parameter (or linewidth-enhancement factor), and the normalized pumping rate expressed as

$$\tau_{st} = \left[\frac{\omega}{\mu^2} \frac{d}{dN_{c0}} \langle \tilde{\chi}_i \rangle A_0^2 \right]^{-1}, \quad (3.9)$$

$$n_{sp} = \langle \tilde{E}_{cv} \rangle / (\langle \tilde{E}_{cv} \rangle - \langle \tilde{E}_{vc} \rangle), \quad (3.10)$$

$$\alpha = \left[\frac{d\langle \tilde{\chi}_r \rangle}{dN_{c0}} \right] / \left[\frac{d\langle \tilde{\chi}_i \rangle}{dN_{c0}} \right], \quad (3.11)$$

and

$$R = p/p_{th} - 1. \quad (3.12)$$

Here p_{th} is the threshold pumping rate.

The power spectra for the noise operators are calculated by the correlation functions. For instance, $\langle |\tilde{\Gamma}_p(\Omega)|^2 \rangle$ is

$$\langle |\tilde{\Gamma}_p(\Omega)|^2 \rangle \equiv 2 \int_{-\infty}^{\infty} \langle \tilde{\Gamma}_p(\tau)\tilde{\Gamma}_p(0) \rangle e^{-j\Omega\tau} d\tau = 2p. \quad (3.13)$$

As indicated in this equation, the power spectrum in this paper is defined as the single-sided (unilateral) spectral density per cps (cycle per second).

Figures 3(a) and (b) are characteristic examples of the normalized amplitude- and phase-noise spectra. The numerical parameters were chosen for a typical semiconductor diode laser. When the pumping level is well above the threshold ($R \gg 1$), the amplitude-noise spectrum becomes Lorentzian

$$P_{\Delta\hat{A}}(\Omega) = \frac{\frac{\omega}{Q}}{\Omega^2 + \left[\frac{\omega}{Q} \right]^2}, \quad R \gg 1 \quad (3.14)$$

which is shown by the dashed curve in Fig. 3(a). The variance of the amplitude is calculated by Parseval's theorem as

$$\langle \Delta\hat{A}^2 \rangle \equiv \int_0^{\infty} \frac{d\Omega}{2\pi} P_{\Delta\hat{A}}(\Omega) = \frac{1}{4}. \quad (3.15)$$

The variance of the photon number is then

$$\langle \Delta\hat{n}^2 \rangle \equiv 4A_0^2 \langle \Delta\hat{A}^2 \rangle = \langle \hat{n} \rangle. \quad (3.16)$$

(3.16) indicates that the internal field features Poissonian photon statistics. Such internal photon statistics cannot be measured by an actual photodetector placed outside the cavity, but are measured by the *Gedankenexperiment* proposed by Scully and Lamb.²⁹

Half of the noise power (3.15) or (3.16) stems from the

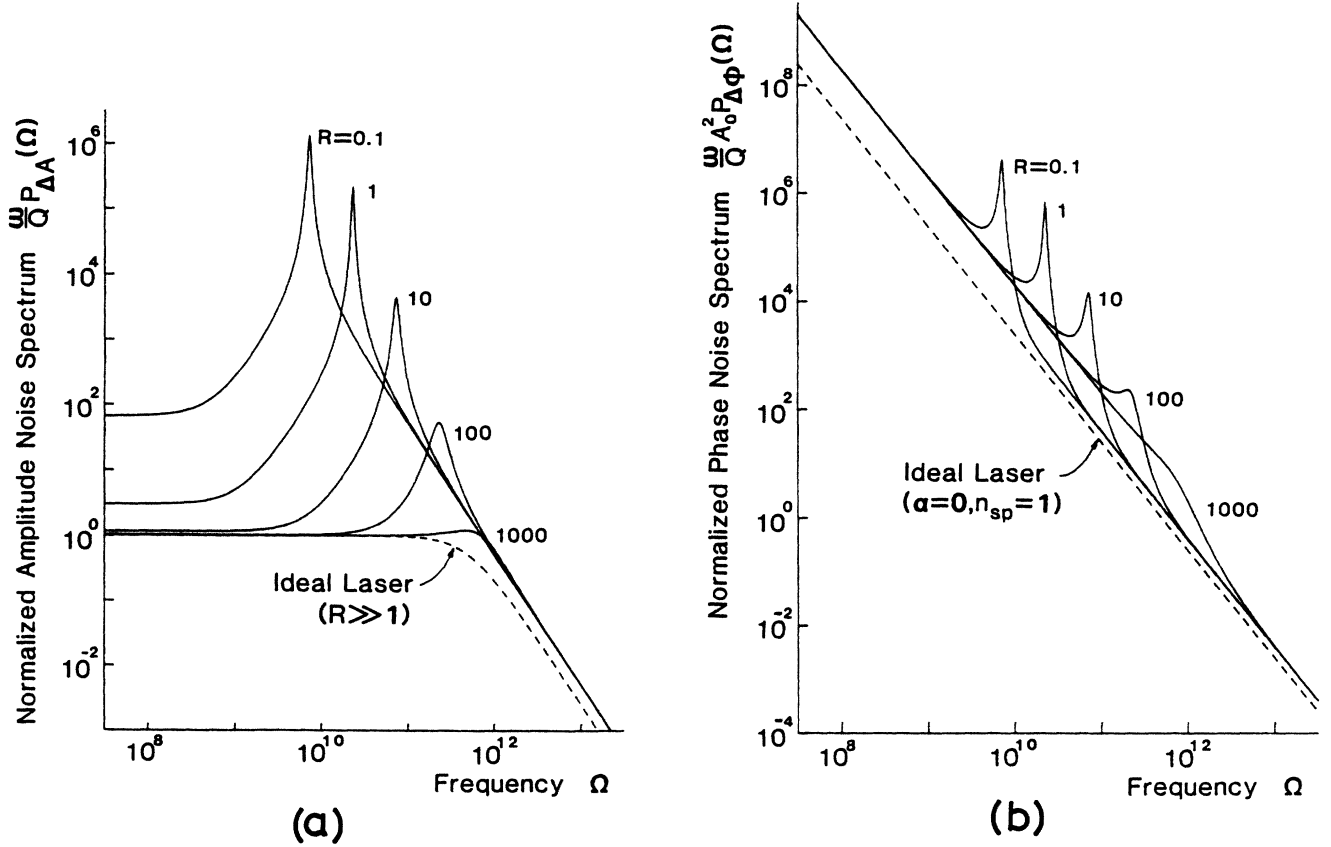


FIG. 3. Normalized amplitude- and phase-noise spectra of a laser internal field. The dotted curves are those for an ideal laser oscillator. Numerical parameters are as follows: $\omega/Q_0 = 10^{11} \text{ s}^{-1}$, $\omega/Q_e = 4 \times 10^{11} \text{ s}^{-1}$, $\alpha = 2$, $n_{sp} = 2$, $\tau_{sp} = 2 \times 10^9 \text{ s}$, and $A_0^2 = 10^5 R$.

pump fluctuation $\tilde{\Gamma}_p$ and the noise operator \hat{g}_r . The remaining half is due to the incident zero-point fluctuation \hat{f}_r . The noise operator $\tilde{\Gamma}_{sp}$ contribution due to the spontaneous decay process is negligible as compared with the pump fluctuation at well above the threshold, since $p \gg \langle \tilde{N}_c \rangle / \tau_{sp}$. The contributions of noise operators \tilde{G}_r and $\tilde{\Gamma}$ cancel each other out exactly because of their negative correlation (2.14).

When the detuning parameter α is equal to zero and the population inversion parameter n_{sp} is equal to unity, the phase-noise spectrum is

$$P_{\Delta \phi}(\Omega) = \frac{\left[\frac{\omega}{Q} \right]}{A_0^2 \Omega^2}, \quad (3.17)$$

which is shown by the dashed curve in Fig. 3(b). Because of the absence of the phase-restoring force, a laser under-

goes the unstationary phase diffusion process which is responsible for the Ω^2 dependence of the noise spectral density. The phase-noise spectrum (3.17) is contributed by the dipole noise operator \tilde{G}_i as well as by the zero-point fluctuations \hat{g}_i and \hat{f}_i . The failure to suppress the \tilde{G}_i contribution is due to the fact that the gain saturation establishes the coherence on only the in-phase component of the dipole moment.

C. Laser oscillator external field

The external output field operator \hat{r} is expressed as

$$\hat{r} = (r_0 + \Delta \hat{r}) e^{-j \Delta \hat{\psi}}, \quad (3.18)$$

where r_0^2 is the average photon flux (number per second), and $\Delta \hat{r}$ and $\Delta \hat{\psi}$ are the Hermitian amplitude and phase operators. The power spectra for $\Delta \hat{r}$ and $\Delta \hat{\psi}$ are (Appendix B)

$$P_{\Delta \hat{r}}(\Omega) = \left\{ \frac{\omega}{Q_e} A_3^2 \langle |\tilde{\Gamma}_p(\Omega)|^2 + |\tilde{\Gamma}_{sp}(\Omega)|^2 + |\tilde{\Gamma}(\Omega)|^2 \rangle + \frac{\omega}{Q_e} (A_1^2 + \Omega^2) \langle |\tilde{G}_r(\Omega)|^2 + |\hat{g}_r(\Omega)|^2 \rangle \right. \\ \left. + \left[\left(\frac{\omega}{Q_e} A_1 - A_2 A_3 - \Omega^2 \right)^2 + \Omega^2 \left(\frac{\omega}{Q_e} + A_1 \right)^2 \right] \frac{\langle |f_r(\Omega)|^2 \rangle}{\frac{\omega}{Q_e}} \right. \\ \left. - 2 \frac{\omega}{Q_e} A_1 A_3 \langle \tilde{\Gamma}(\Omega) \tilde{G}_r(\Omega) \rangle \right\} [(A_2 A_3 + \Omega^2)^2 + A_1^2 \Omega^2]^{-1}, \quad (3.19)$$

and

$$P_{\Delta\hat{\psi}}(\Omega) = \frac{\left[\frac{\omega}{Q_e}\right]}{r_0^2} \left\{ \frac{1}{\left[\frac{\omega}{Q_e}\right]^2 + \Omega^2} \langle |\hat{f}_i(\Omega)|^2 \rangle + \frac{\left[\frac{\omega}{Q_e}\right]}{r_0^2 \Omega^2} \langle |\tilde{G}_i(\Omega)|^2 + |\hat{g}_i(\Omega)|^2 \rangle \right. \\ \left. + \left[\frac{A_2}{\Omega}\right]^2 \langle |\tilde{G}_r(\Omega)|^2 + |\hat{g}_r(\Omega)|^2 + |\hat{f}_r(\Omega)|^2 \rangle [(\Omega^2 + A_2 A_3)^2 + \Omega^2 A_1^2]^{-1} \right\}. \quad (3.20)$$

Figures 4(a) and 4(b) are characteristic examples of the amplitude and normalized phase-noise spectra for the external field. Numerical parameters are the same as for Fig. 3. When the pumping level is at well above the threshold ($R \gg 1$), the amplitude-noise spectrum becomes white,

$$P_{\Delta\hat{r}}(\Omega) = \frac{1}{2}, \quad R \gg 1 \quad (3.21)$$

which is shown by the dashed line in Fig. 4(a). The power spectrum for the photon flux noise, $\Delta\hat{N} = \Delta(\hat{r}^\dagger \hat{r})$, in such a pumping level is equal to

$$P_{\Delta\hat{N}}(\Omega) \equiv 4r_0^2 P_{\Delta\hat{r}}(\Omega) = 2\langle \hat{N} \rangle. \quad (3.22)$$

This shot-noise-limited white-noise spectrum is that which is measured by an actual photodetector placed outside the cavity.

The amplitude-noise spectrum $P_{\Delta\hat{r}}(\Omega \leq \omega/Q)$ within the cavity bandwidth is due to the pump fluctuation $\tilde{\Gamma}_p$

and the (internal-loss-induced) noise operator \hat{g}_r . The amplitude-noise spectrum $P_{\Delta\hat{r}}(\Omega \geq \omega/Q)$ above the cavity bandwidth, on the other hand, stems from the reflected zero-point fluctuation \hat{f}_e . This was schematically shown in Fig. 5. Also as mentioned, one-half of the internal amplitude-noise spectrum, $P_{\Delta\hat{r}}(\Omega)$, is contributed by the incident zero-point fluctuation \hat{f}_r . This part of the internal amplitude noise is completely suppressed when the internal field is coupled out of the cavity, because the reflected zero-point fluctuation \hat{f}_e beats against the coherent excitation r_0 and the resulting amplitude noise is the exact replica of the internal amplitude noise due to \hat{f}_r . Because of the minus sign in front of \hat{f}_e in (2.9), the two amplitude noises are 180° out of phase and cancel each other out exactly. As a result of this destructive interference, the remaining half of the internal amplitude noise due to $\tilde{\Gamma}_p$ and \hat{g}_r emerges in the external output field. In the frequency region higher than the cavity bandwidth ($\Omega \geq \omega/Q$), the internal amplitude noise is cut off as

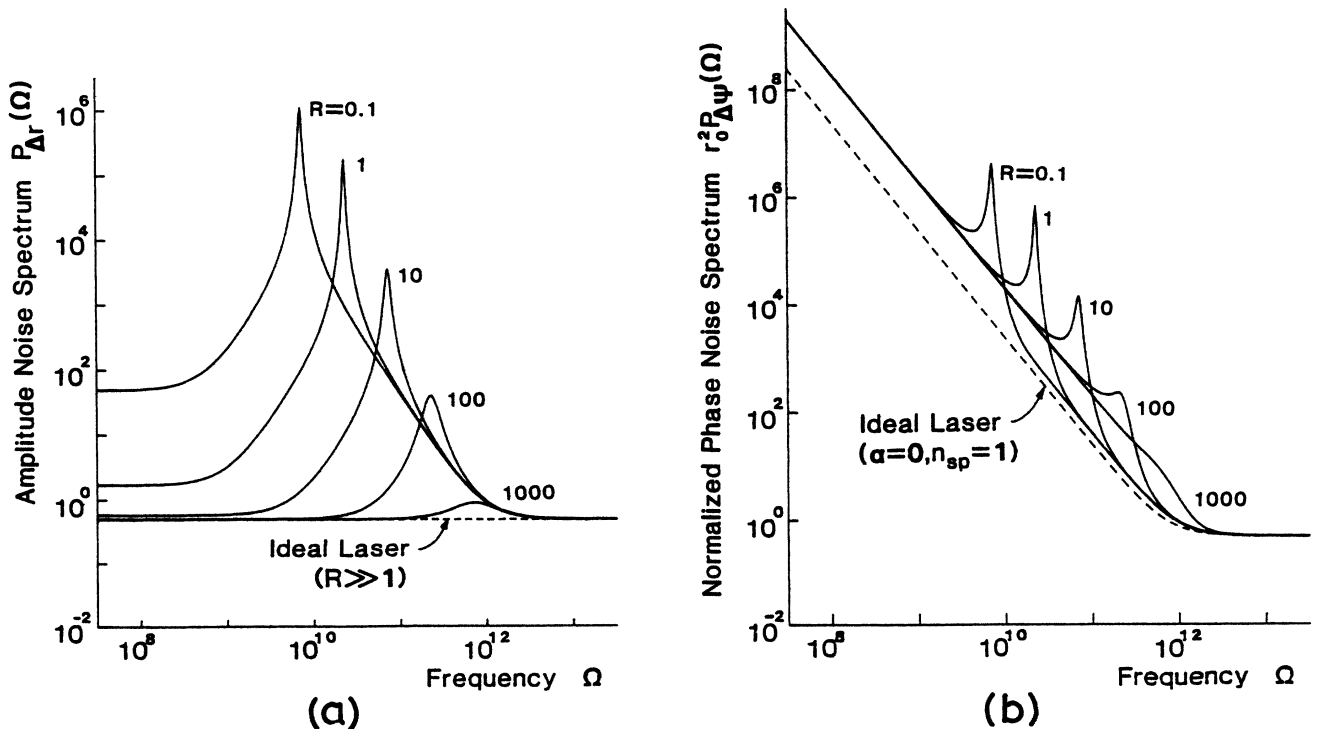


FIG. 4. Amplitude- and normalized phase-noise spectra of a laser external field. The dotted curves are those for an ideal laser. Numerical parameters are the same as those in Fig. 3.

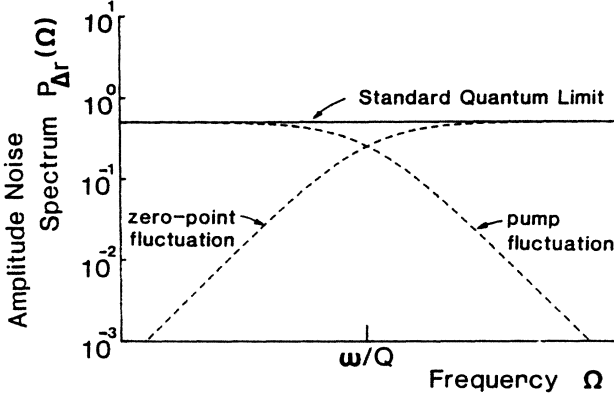


FIG. 5. Origins for standard quantum-limited amplitude-noise spectrum of a laser oscillator.

shown in Fig. 3(a), while the incident zero-point fluctuation is simply reflected back from the mirror. This reflected zero-point fluctuation constitutes the higher-frequency part of the white amplitude noise.

When α is zero and n_{sp} is unity, the phase-noise spectrum of the external field is

$$P_{\Delta\hat{\psi}}(\Omega) = \frac{1}{2r_0^2} + \frac{\omega}{A_0^2\Omega^2} = \frac{1}{2r_0^2} + \frac{Q_e}{r_0^2\Omega^2}, \quad (3.23)$$

which is shown by the dashed curve in Fig. 4(b). The external phase-noise spectrum is different from the internal phase-noise spectrum (3.17) only by the first term of (3.23). This term is due to the reflected zero-point fluctuation. The destructive interference between the transmitted internal field and the reflected zero-point fluctuation, which suppresses the amplitude-noise spectrum within the cavity bandwidth, does not work for the phase-noise spectrum within the cavity bandwidth. This is because the internal phase noise $\Delta\hat{\phi}$ due to the incident zero-point fluctuation, the first term of (B2), is just in the quadrature phase with the phase noise due to the reflected zero-point fluctuation, the second term of (B2). Therefore, the two noise powers are additive, even though they originate from the same noise source \hat{f}_e .

D. The minimum-uncertainty relation

The commutation relation for the external field \hat{r} having a continuous spectrum (broadband) is defined in terms of its Fourier component,³⁰

$$[\hat{r}(\Omega), \hat{r}^\dagger(\Omega')] = \delta(\Omega - \Omega'). \quad (3.24)$$

Here we assume the decomposition for $\hat{r}(t)$ as

$$\hat{r}(t) = \int_{-\infty}^{\infty} \hat{r}(\Omega) e^{-j\Omega t} d\Omega. \quad (3.25)$$

If we assign the amplitude noise $\Delta\hat{r}$ and phase noise $\Delta\hat{\psi}$ to the two quadrature noise components $\Delta\hat{r}_1$ and $\Delta\hat{r}_2$, indicated in Fig. 6, that is,

$$\Delta\hat{r} = \Delta\hat{r}_1,$$

and

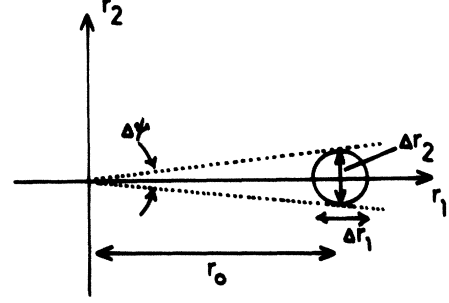


FIG. 6. Two quadrature-noise components, $\Delta\hat{r}_1$ and $\Delta\hat{r}_2$, of an external field and the corresponding amplitude $\Delta\hat{r}$ and phase noise $\Delta\hat{\psi}$.

$$\Delta\hat{\psi} = -\frac{\Delta\hat{r}_2}{r_0},$$

(3.24) can be rewritten as

$$[\Delta\hat{r}(\Omega), \Delta\hat{\psi}(\Omega')] = -\frac{j}{2r_0} \delta(\Omega - \Omega'). \quad (3.26)$$

As shown already in Appendix A, the frequency component $\hat{r}(\Omega)$ is obtained from a Fourier-series analysis with a period T . We renormalize $\hat{r}(\Omega)$ using the relation

$$\hat{r}_k = \sqrt{2\pi/T} \hat{r}(\Omega_k) \quad (3.27)$$

We may then write (3.24) and (3.26) in the forms

$$[\hat{r}_k, \hat{r}_{k'}^\dagger] = \delta_{kk'}. \quad (3.24')$$

and

$$[\Delta\hat{r}_k, \Delta\hat{\psi}_{k'}] = -\frac{j}{2r_0} \delta_{kk'}. \quad (3.26')$$

The Dirac δ function is identified by the Kronecker δ function and vice versa,

$$\delta(\Omega_k - \Omega_{k'}) \leftrightarrow \frac{\delta_{kk'}}{\left[\frac{2\pi}{T} \right]}.$$

The spectrum of $\Delta\hat{r}$ can be calculated conveniently by $\Delta\hat{r}_k$,

$$P_{\Delta\hat{r}}(\Omega_k) = \int \langle \Delta\hat{r}(\Omega_k) \Delta\hat{r}(\Omega'_k) \rangle d\Omega'_k = \langle \Delta\hat{r}_k^2 \rangle. \quad (3.28)$$

From the commutation relation (3.26') the minimum-uncertainty product for the amplitude and phase-noise spectra results in

$$P_{\Delta\hat{r}}(\Omega_k) P_{\Delta\hat{\psi}}(\Omega_k) = \langle \Delta\hat{r}_k^2 \rangle \langle \Delta\hat{\psi}_k^2 \rangle = \frac{1}{4r_0^2}. \quad (3.29)$$

It is obvious from (3.21) and (3.23) [or from the dashed curves in Figs. 4(a) and (b)] that the amplitude- and phase-noise spectra of an ideal laser satisfies the minimum-uncertainty product (3.29) in the frequency region above the cavity bandwidth, $\Omega \geq \omega/Q$. The product of the amplitude- and phase-noise spectra in the frequency region within the cavity bandwidth, $\Omega \leq \omega/Q$, is larger than the minimum-uncertainty product (3.29), however, because of the phase diffusion noise. An ordinary laser

oscillator is not really a truly quantum-limited device in this respect, even though the conditions of $R \gg 1$, $\alpha=0$, and $n_{sp}=1$ are all satisfied.

In other words, the possibility exists for improving the amplitude noise below the standard quantum limit in the frequency region within the cavity bandwidth. The discussion in this section suggests that such improvement is indeed possible if the pump fluctuation and the internal loss can be eliminated.

IV. POSSIBLE SCHEMES FOR SUPPRESSING PUMP FLUCTUATION

As discussed in Sec. II, pump amplitude fluctuation can be suppressed if the pump light is sub-Poissonian light or near-photon-number state light in an optical pumping scheme. This trivial solution as to how to suppress the pump fluctuation is not interesting from a practical viewpoint. This is because intense sub-Poissonian light is not presently available, even though phase coherency is not required for this purpose.

One possible scheme for suppressing pump fluctuation is the use of an electron beam in a space-charge-limited vacuum tube, as shown in Fig. 7(a). When the electron-emission rate increases above its average rate, the number of space charges increases and the potential minimum between the cathode and the anode becomes more negative due to the Coulomb repulsion between the "crowded" space electrons as shown in Fig. 7(b). Therefore more electrons return back to the cathode due to their insufficient initial velocity, $v \leq (2qE_m/m)^{1/2}$, where E_m is the minimum potential and m is an electron mass. When the electron-emission rate decreases below its average rate, the potential minimum becomes less negative. This deformation of the potential profile contributes to decreasing the

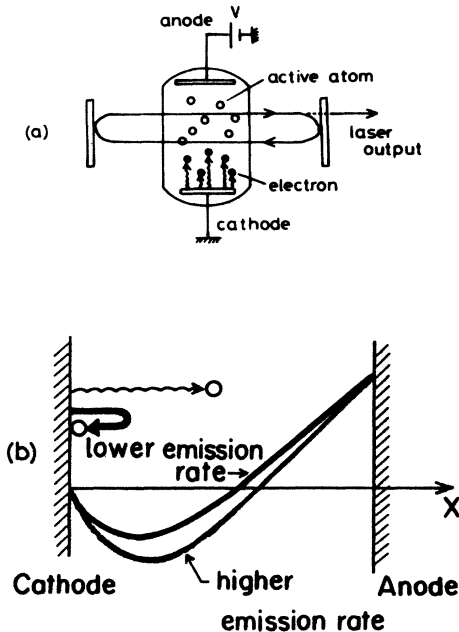


FIG. 7. Possible schemes for suppressing pump fluctuation. (a) A laser oscillator including space-charge-limited electrons in a vacuum tube. (b) Potential distributions between a cathode and an anode.

number of electrons returning back to the cathode. It is known that the electron arrival process at the anode is Poissonian and the anode current features shot noise in a temperature-limited vacuum tube. In a space-charge-limited vacuum tube, however, the electron-arrival process and the anode current are regulated below such limits because of the above-mentioned mechanism.³¹ Actually, the variance of the arrival-electron number and the anode current can be considerably decreased below the usual Poisson limit and shot-noise level.

If active atoms are sealed in a vacuum tube and are excited by such sub-Poissonian electrons as shown in Fig. 7(a), the pump fluctuation of this laser can certainly be held below the ordinary shot-noise level. This is essentially the stimulated emission version of the (spontaneous) Franck-Hertz effect.³² In fact, Teich and Saleh observed sub-Poissonian photon statistics in the spontaneous light from their space-charge-limited vacuum tube containing Hg atoms.³³ The sub-Poissonian statistics in pumped electrons were imparted to the statistics in the spontaneously emitted photons in their experiment. In principle, the same effect can be carried over to a laser oscillator.

Figure 8 shows the injection-current-pumped semiconductor laser, where the carrier-injection process is regulated by a similar effect.¹⁹ The carrier-injection rate, that is, the diode junction current, is determined by the forward-biased voltage across a $p-n$ junction. The junction voltage counteracts the built-in potential in a depletion layer and makes the carrier-diffusion process dominating over the reverse-directed drift process. When the junction current increases above its average rate, the junction voltage decreases due to the increase in voltage across the series resistance R_s . Therefore, more minority carriers (electrons in the case of Fig. 8) return back to the n -type bulk layer due to the dominating built-in field in a depletion region. When the injection current decreases below its average rate, the junction voltage increases and more electrons

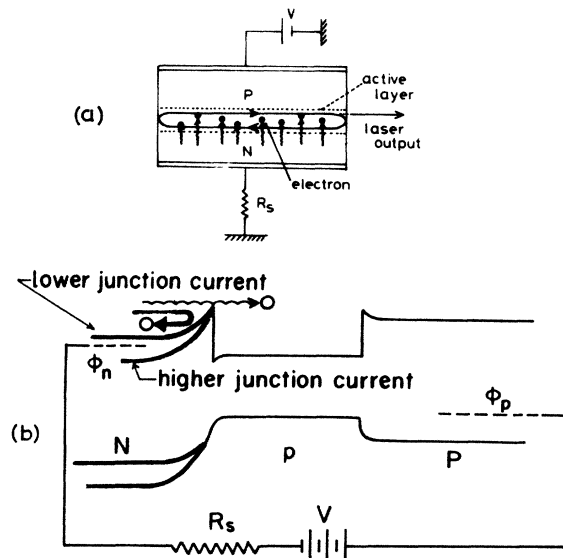


FIG. 8. Possible schemes for suppressing pump fluctuation. (a) A semiconductor laser pumped by a high-impedance source. (b) Energy-band diagrams of a $n-p-p$ double heterojunction.

can diffuse into an active layer. This junction-voltage modulation effect induced by the presence of the series resistance contributes to the regulation of the process of minority carrier injection into the active layer.

In a forthcoming paper²⁰ we will discuss this problem in detail. The microscopic theory of junction-current noise based on the minority carrier-transport process in an active layer is developed, which accounts for both the thermal fluctuation of minority carrier flow and the quantum-mechanical generation-recombination noise of minority carriers. The noise-equivalent circuit reveals that the pump fluctuation of a semiconductor laser is not a usual shot-noise-limited one but the thermal noise generated in the resistance R_s . It can be suppressed by the large R_s value.

An important feature of the scheme shown in Fig. 8 is the achievable high quantum (conversion) efficiency. Most of the injected electrons into the active layer can be converted to the emitted coherent photons from the laser cavity. An ordinary semiconductor laser possesses a quantum efficiency of higher than 0.8, i.e., more than 80% of the injected electrons are emitted from the laser as coherent radiation. This feature prevents the amplitude squeezing (or sub-Poissonian features) of the emitted photons from being diluted by the random deletion (partition) noise. For the purpose of the present paper, it is sufficient to note that pump-fluctuation suppression is basically possible using one of these principles.

V. QUANTUM-MECHANICAL CONSISTENCY OF A PUMP-NOISE-SUPPRESSED LASER

Before discussing the details of the amplitude- and phase-noise spectra of a pump-noise-suppressed laser oscillator, we will here discuss that the absence of the pump fluctuation does not violate quantum-mechanical consistency. For this purpose, let us introduce the two-photon formalism for a broadband squeezed state.^{12,34} We assume here the fluctuation frequency Ω is much lower than the optical frequency ω , so that $(\omega \pm \Omega)/\omega \simeq 1$.

A. Commutator-bracket preservation for internal field

Quantum-mechanical consistency requires that the proper commutation relations hold for both the internal field \hat{A} and the external field $\hat{\gamma}$. The internal field \hat{A} should preserve the commutator bracket (2.4) for a "discrete" mode. $\hat{A}(t)$ is expressed in terms of its positive frequency part $\hat{a}_+(\Omega)$ at $\omega + \Omega$, and negative frequency part $\hat{a}_-(\Omega)$ at $\omega - \Omega$, such that

$$\hat{A}(t) = \int_0^\infty [\hat{a}_+(\Omega)e^{-j\Omega t} + \hat{a}_-(\Omega)e^{j\Omega t}]d\Omega. \quad (5.1)$$

If $\hat{a}_+(\Omega)$ and $\hat{a}_-(\Omega)$ are normalized in a similar way as (3.27),

$$\hat{a}_{+k} = \sqrt{2\pi/T} \hat{a}_+(\Omega_k), \quad (5.2a)$$

$$\hat{a}_{-k} = \sqrt{2\pi/T} \hat{a}_-(\Omega_k), \quad (5.2b)$$

(5.1) becomes

$$\hat{A}(t) = \sum_k \sqrt{2\pi/T} (\hat{a}_{+k} e^{-j\Omega_k t} + \hat{a}_{-k} e^{j\Omega_k t}). \quad (5.3)$$

The commutator bracket (2.4) can then be rewritten as

$$\begin{aligned} & [\hat{A}(t), \hat{A}^\dagger(t)] \\ &= \sum_k \frac{2\pi}{T} \{[\hat{a}_{+k}, \hat{a}_{+k}^\dagger] + [\hat{a}_{-k}, \hat{a}_{-k}^\dagger]\} \\ &= \int_0^\infty [\hat{a}_{+k}, \hat{a}_{+k}^\dagger] d\Omega_k + \int_0^\infty [\hat{a}_{-k}, \hat{a}_{-k}^\dagger] d\Omega_k \\ &= 1. \end{aligned} \quad (5.4)$$

Here the second equality assumes $\Delta\Omega_k = 2\pi/T$, and the summation is replaced by the integral in the limit of $T \rightarrow \infty$.

Our task in this section is to prove (5.4) without the necessity for the pump fluctuation $\tilde{\Gamma}_p$. The amplitude and normalized phase noise in (3.5a) can be assigned as the two quadrature noise components

$$\hat{A}(t) = A_0 + \hat{a}_1(t) + j\hat{a}_2(t), \quad (5.5)$$

where

$$\hat{a}_1(t) = \Delta\hat{A}(t) \quad (\text{amplitude noise}),$$

and

$$\hat{a}_2(t) = -A_0\Delta\hat{\phi}(t) \quad (\text{normalized phase noise}).$$

If the population-difference decay rate, $1/\tau_c = 1/\tau_{sp} + 1/\tau_{st}$ is much larger than the photon decay rate ω/Q , the population-difference fluctuating operator $\Delta\tilde{N}_c$ can be eliminated adiabatically from the Langevin equations (A1)–(A3). The condition $1/\tau_c \gg \omega/Q$ is always satisfied at a high pumping level $R \gg 1$, even though the spontaneous decay rate $1/\tau_{sp}$ is smaller than ω/Q as in the case of a semiconductor laser. Because we are interested in this operational region ($R \gg 1$), we will confine our discussion to it.

The population-difference operator $\Delta\tilde{N}_c$ is obtained from (A3), such that

$$\begin{aligned} \Delta\tilde{N}_c &= \left[\frac{1}{\tau_{sp}} + \frac{1}{\tau_{st}} \right]^{-1} \left[-2 \left[\frac{\omega}{Q} \right] A_0 \hat{a}_1 + \tilde{\Gamma}_p + \tilde{\Gamma}_{sp} + \tilde{\Gamma} \right] \\ &\simeq \tau_{st} \left[-2 \left[\frac{\omega}{Q} \right] A_0 \hat{a}_1 + \tilde{\Gamma} \right]. \end{aligned} \quad (5.6)$$

Here, the second equality assumes that the spontaneous decay rate is much smaller than the stimulated decay rate, and that the pump fluctuation is suppressed by some of the schemes discussed in Sec. IV. Using (5.6) in (A1) and (A2), we obtain the equations of motion for the two quadrature components as

$$\frac{d}{dt} \hat{a}_1 = -\frac{\omega}{Q} \hat{a}_1 + \frac{\tilde{\Gamma}}{2A_0} + \tilde{G}_1 + \hat{g}_1 + \hat{f}_1, \quad (5.7)$$

and

$$\frac{d}{dt} \hat{a}_2 = \tilde{G}_2 + \hat{g}_2 + \hat{f}_2. \quad (5.8)$$

\tilde{G}_1 , \tilde{G}_2 , \hat{g}_1 , and \hat{g}_2 are given by equations similar to (B5)

and (B6) for \hat{f}_1 and \hat{f}_2 .

The positive and negative frequency component operators are defined by

$$\hat{a}_+ = \hat{a}_1 + j\hat{a}_2, \quad (5.9)$$

and

$$\hat{a}_-^\dagger = \hat{a}_1 - j\hat{a}_2. \quad (5.10)$$

From (5.7)–(5.10) we obtain

$$\frac{d}{dt}\hat{a}_+ = -\frac{1}{2}\frac{\omega}{Q}(\hat{a}_+ + \hat{a}_-^\dagger) + n_+, \quad (5.11)$$

and

$$\frac{d}{dt}\hat{a}_-^\dagger = -\frac{1}{2}\frac{\omega}{Q}(\hat{a}_-^\dagger + \hat{a}_+) + n_-^\dagger. \quad (5.12)$$

Here, the new noise operators are given by

$$n_+ = \frac{\tilde{\Gamma}}{2A_0} + (\tilde{G} + \hat{g} + \hat{f})e^{j\Delta\hat{\phi}}, \quad (5.13)$$

and

$$n_-^\dagger = \frac{\tilde{\Gamma}}{2A_0} + e^{-j\Delta\hat{\phi}}(\tilde{G}^\dagger + \hat{g}^\dagger + \hat{f}^\dagger). \quad (5.14)$$

The Fourier transform of (5.11) and (5.12) and the relation (5.2) results in

$$\hat{a}_{+k} = \frac{\left[-j\Omega + \frac{1}{2}\left(\frac{\omega}{Q}\right)\right]n_{+k} - \frac{1}{2}\frac{\omega}{Q}n_{-k}^\dagger}{-\Omega^2 - j\Omega\left(\frac{\omega}{Q}\right)}, \quad (5.15)$$

and a similar equation for \hat{a}_{-k}^\dagger . The commutator bracket density integrated over all frequencies then becomes

$$\begin{aligned} \hat{r}_{+k} &= -\hat{f}_{e,+k} + (\omega/Q_e)^{1/2}\hat{a}_{+k} \\ &= \frac{\left[\Omega^2 + j\Omega\left(\frac{\omega}{Q}\right)\right]\hat{f}_{e,+k} + (\omega/Q_e)^{1/2}\left[-j\Omega + \frac{1}{2}\left(\frac{\omega}{Q}\right)\right]\hat{n}_{+k} - \frac{1}{2}\left(\frac{\omega}{Q}\right)(\omega/Q_e)^{1/2}\hat{n}_{-k}^\dagger}{-\Omega^2 - j\Omega\left(\frac{\omega}{Q}\right)}. \end{aligned} \quad (5.22)$$

If we then use the commutator bracket for the noise operator $\hat{f}_{e,+k} = \sqrt{2\pi/T}f_{e,+}(\Omega_k)$,

$$[\hat{f}_{e,+k}, \hat{f}_{e,+k}^\dagger] = \delta_{kk'}, \quad (5.23)$$

and

$$[\hat{f}_{e,+k}, n_{+k}^\dagger] = [n_{+k}, \hat{f}_{e,+k}^\dagger] = (\omega/Q_e)^{1/2}\delta_{kk'}, \quad (5.24)$$

we immediately find

$$[\hat{r}_{+k}, \hat{r}_{+k}^\dagger] = \delta_{kk'}. \quad (5.25)$$

$$\begin{aligned} &\int_0^\infty \{[\hat{a}_{+k}, \hat{a}_{+k}^\dagger] + [\hat{a}_{-k}, \hat{a}_{-k}^\dagger]\} d\Omega_k \\ &= \int_0^\infty \left\{ \frac{[n_{+k}, n_{+k}^\dagger]}{\left[\Omega_k^2 + \left(\frac{\omega}{Q}\right)\right]^2} + \frac{[n_{-k}, n_{-k}^\dagger]}{\left[\Omega_k^2 + \left(\frac{\omega}{Q}\right)\right]^2} \right\} d\Omega_k = 1. \end{aligned} \quad (5.16)$$

Here we used the relations

$$[n_{+k}, n_{+k}^\dagger] = [n_{-k}, n_{-k}^\dagger] = \frac{\omega}{Q}\delta_{kk'} \quad (5.17)$$

and

$$[n_{+k}, n_{+k'}] = [n_{-k}, n_{-k'}] = 0 \quad (5.18)$$

for $n_{+k} = \sqrt{2\pi/T}n_+(\Omega_k)$ and $n_{-k} = \sqrt{2\pi/T}n_-(\Omega_k)$. The derivation of (5.17) is based on (2.5)–(2.7), (2.13), and (2.14).

B. Commutator bracket preservation for external field

The external field $\hat{r}(t)$ is similarly decomposed into its positive frequency part $\hat{r}_+(\Omega)$ at $\omega + \Omega$, and negative frequency part $\hat{r}_-(\Omega)$ at $\omega - \Omega$, such that

$$\begin{aligned} \hat{r}(t) &= \int_0^\infty [\hat{r}_+(\Omega)e^{-j\Omega t} + \hat{r}_-(\Omega)e^{j\Omega t}] d\Omega \\ &= \sum_k \sqrt{2\pi/T} [\hat{r}_{+k}e^{-j\Omega_k t} + \hat{r}_{-k}e^{j\Omega_k t}]. \end{aligned} \quad (5.19)$$

The proper commutator bracket for the external field is given by³⁰

$$[\hat{r}_+(\Omega), \hat{r}_+(\Omega')] = [\hat{r}_-(\Omega), \hat{r}_-(\Omega')] = \delta(\Omega - \Omega'), \quad (5.20)$$

or equivalently by

$$[\hat{r}_{+k}, \hat{r}_{+k'}^\dagger] = [\hat{r}_{-k}, \hat{r}_{-k'}^\dagger] = \delta_{kk'}. \quad (5.21)$$

Using (5.3) and (5.19) in (2.9), we obtain the positive frequency component of $\hat{r}(t)$ as

VI. CAVITY DEGENERATE PARAMETRIC AMPLIFIER VERSUS PUMP-NOISE-SUPPRESSED LASER

A cavity degenerate parametric amplifier is the simplest model for a state squeezer. A pump-noise-suppressed laser oscillator features similar performances, even though the squeezing direction of the field is different from that of the cavity degenerate paramp as shown in Fig. 1. When the noise distribution is small as compared with the coherent excitation, however, the difference between a

squeezed state and an amplitude-squeezed state is negligible. Therefore it is interesting to compare these two devices from the viewpoint of quantum limit.

A. Cavity-degenerate parametric amplifier

Let us consider the cavity degenerate parametric amplifier shown in Fig. 9. The in-phase and quadrature amplitudes of the internal field obey the equations,¹²

$$\frac{d}{dt}\hat{a}_1 = -\left[\frac{1}{2}\frac{\omega}{Q_e} + \frac{1}{\tau_1^0}\right]\hat{a}_1 + (\omega/Q_e)^{1/2}\hat{b}_1 \quad (6.1)$$

and

$$\frac{d}{dt}\hat{a}_2 = -\left[\frac{1}{2}\frac{\omega}{Q_e} + \frac{1}{\tau_2^0}\right]\hat{a}_2 + (\omega/Q_e)^{1/2}\hat{b}_2. \quad (6.2)$$

Here \hat{a}_1 and \hat{a}_2 are defined by (5.5), and $1/\tau_1^0$ and $1/\tau_2^0$ are the amplification and deamplification rates which satisfy

$$\frac{1}{\tau_1^0} + \frac{1}{\tau_2^0} = 0 \quad (6.3)$$

for a degenerate parametric amplifier.^{3,12} There is no internal noise source required such as the dipole-moment fluctuation operator if (6.3) is satisfied.²⁷ For the purpose of comparing with a pump-noise-suppressed laser, we assume the phase of a pump wave is adjusted to satisfy

$$\frac{1}{\tau_1^0} = -\frac{1}{\tau_2^0} > 0,$$

that is, the in-phase amplitude \hat{a}_1 is deamplified and the quadrature amplitude \hat{a}_2 is amplified. \hat{b}_1 and \hat{b}_2 are the in-phase and quadrature amplitude of an input signal \hat{b}_e . We assumed that the cavity internal loss is negligible.

The in-phase and quadrature-noise spectra calculated from (6.1) and (6.2) are given by

$$P_{\hat{a}_1}(\Omega) = \frac{\frac{1}{2}\left[\frac{\omega}{Q_e}\right]}{\Omega^2 + \left[\frac{1}{2}\frac{\omega}{Q_e} + \frac{1}{\tau_1^0}\right]^2} \rightarrow \frac{\frac{1}{2}\left[\frac{\omega}{Q_e}\right]}{\Omega^2 + \left[\frac{\omega}{Q_e}\right]^2},$$

as $\left[\frac{1}{\tau_1^0} \rightarrow \frac{1}{2}\frac{\omega}{Q_e}\right]$ (6.4)

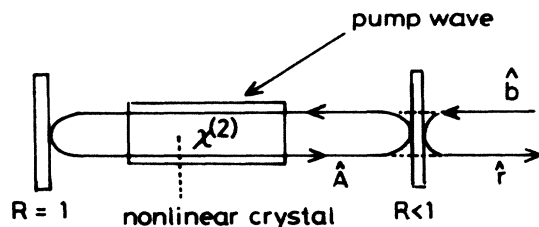


FIG. 9. Cavity degenerate parametric amplifier.

and

$$P_{\hat{a}_2}(\Omega) = \frac{\frac{1}{2}\left[\frac{\omega}{Q_e}\right]}{\Omega^2 + \left[\frac{1}{2}\frac{\omega}{Q_e} + \frac{1}{\tau_2^0}\right]^2} \rightarrow \frac{\left[\frac{\omega}{Q_e}\right]}{2\Omega^2},$$

as $\left[-\frac{1}{\tau_2^0} \rightarrow \frac{1}{2}\frac{\omega}{Q_e}\right]$ (6.5)

when the input signal is a broadband coherent state, $P_{\hat{b}_1}(\Omega) = P_{\hat{b}_2}(\Omega) = \frac{1}{2}$. Figure 10 shows characteristic examples of $P_{\hat{a}_1}(\Omega)$ and $P_{\hat{a}_2}(\Omega)$ as a function of $(1/\tau_1^0)^{1/2}(\omega/Q_e)$. The maximum reduction of the in-phase noise spectrum is achieved at the oscillation threshold $1/\tau_1^0 \approx \frac{1}{2}(\omega/Q_e)$. The variance in the in-phase amplitude $\langle \Delta \hat{a}_1^2 \rangle \equiv \int_0^\infty (d\Omega/2\pi) P_{\hat{a}_1}(\Omega)$ is $\frac{1}{4}$ for an empty cavity ($1/\tau_1^0 = 0$), and is $\frac{1}{8}$ at the oscillation threshold [$1/\tau_1^0 = \frac{1}{2}(\omega/Q_e)$]. The squeezing factor is only one-half for the internal field, which is also discovered by the Fokker-Planck equation treatment.³⁵

If we adopt the relation between the input and output signals,

$$\hat{r} = -\hat{b}_e + (\omega/Q_e)^{1/2}\hat{A}, \quad (6.6)$$

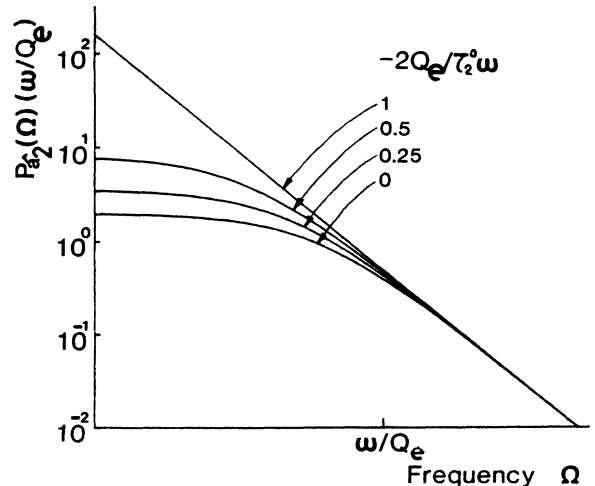
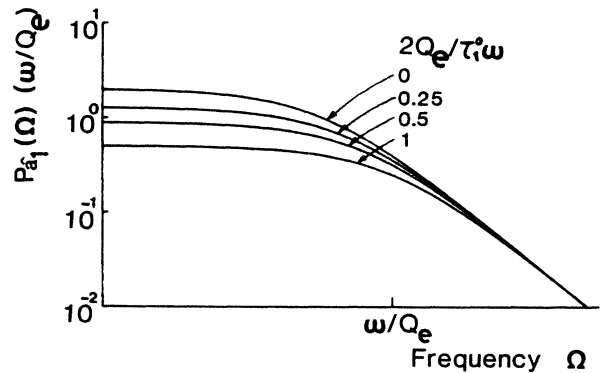


FIG. 10. In-phase and quadrature-noise spectra of an internal field in a cavity degenerate parametric amplifier.

the in-phase and quadrature noise spectra of the output signal can be obtained as follows:

$$P_{\hat{r}_1}(\Omega) = \frac{1}{2} \frac{\Omega^2 + \left[\frac{1}{2} \frac{\omega}{Q_e} - \frac{1}{\tau_1^0} \right]^2}{\Omega^2 + \left[\frac{1}{2} \frac{\omega}{Q_e} + \frac{1}{\tau_1^0} \right]^2} \rightarrow \frac{1}{2} \frac{\Omega^2}{\Omega^2 + \left[\frac{\omega}{Q_e} \right]^2},$$

as $\left[\frac{1}{\tau_1^0} \rightarrow \frac{1}{2} \frac{\omega}{Q_e} \right]$ (6.7)

$$P_{\hat{r}_2}(\Omega) = \frac{1}{2} \frac{\Omega^2 + \left[\frac{1}{2} \frac{\omega}{Q_e} - \frac{1}{\tau_2^0} \right]^2}{\Omega^2 + \left[\frac{1}{2} \frac{\omega}{Q_e} + \frac{1}{\tau_2^0} \right]^2} \rightarrow \frac{1}{2} \frac{\Omega^2 + \left[\frac{\omega}{Q_e} \right]^2}{\Omega^2},$$

as $\left[-\frac{1}{\tau_2^0} \rightarrow \frac{1}{2} \frac{\omega}{Q_e} \right]$. (6.8)

Characteristic examples of $P_{\hat{r}_1}(\Omega)$ and $P_{\hat{r}_2}(\Omega)$ are shown in Fig. 11 as a function of $(1/\tau_1^0)/\frac{1}{2}(\omega/Q_e)$. Equations (6.7) and (6.8) satisfy the minimum-uncertainty product discussed in Sec. III.

Using (5.9) and (5.10) in (6.1) and (6.2), we obtain

$$\frac{d}{dt} \hat{a}_+ = -\frac{1}{2} \frac{\omega}{Q_e} \hat{a}_+ - \frac{1}{2} \left[\frac{1}{\tau_1^0} - \frac{1}{\tau_2^0} \right] \hat{a}_-^\dagger + (\omega/Q_e)^{1/2} \hat{b}_+,$$

(6.9)

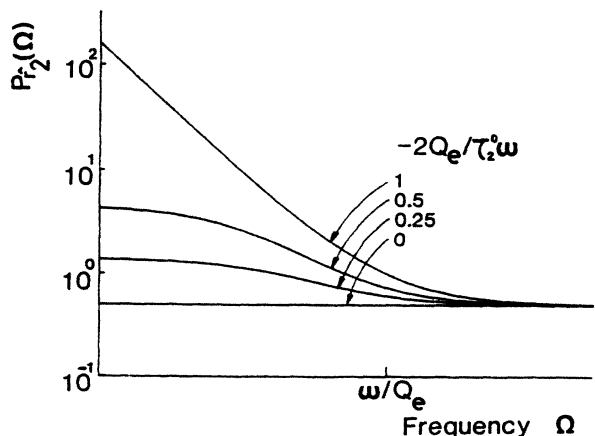
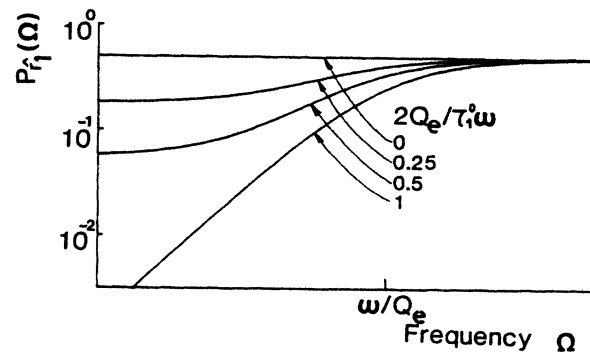


FIG. 11. In-phase and quadrature-noise spectra of an output field from a cavity degenerate parametric amplifier.

and

$$\frac{d}{dt} \hat{a}_-^\dagger = -\frac{1}{2} \frac{\omega}{Q_e} \hat{a}_-^\dagger - \frac{1}{2} \left[\frac{1}{\tau_1^0} - \frac{1}{\tau_2^0} \right] \hat{a}_+ + (\omega/Q_e)^{1/2} \hat{b}_-^\dagger.$$

(6.10)

Here $\hat{b}_+ = \hat{b}_1 + j\hat{b}_2$ and $\hat{b}_-^\dagger = \hat{b}_1 - j\hat{b}_2$. If the input signal has a bandwidth much narrower than the amplifier bandwidth, $B \cong \frac{1}{2}(\omega/Q_e) - 1/\tau_1^0$, a single-mode description of the system simplifies the analysis. The input and output signal modes \hat{b}_{s+} and \hat{r}_{s+} are related by

$$\hat{r}_{s+} = -\hat{b}_{s+} + (\omega/Q_e)^{1/2} \hat{a}_{s+}$$

$$= \frac{\left[\frac{\omega}{Q_e} \right]^2 + \left[\frac{1}{\tau_1^0} - \frac{1}{\tau_2^0} \right]^2}{\left[\frac{\omega}{Q_e} \right]^2 - \left[\frac{1}{\tau_1^0} - \frac{1}{\tau_2^0} \right]^2} \hat{b}_{s+}$$

$$- \frac{2 \left[\frac{\omega}{Q_e} \right] \left[\frac{1}{\tau_1^0} - \frac{1}{\tau_2^0} \right]}{\left[\frac{\omega}{Q_e} \right]^2 - \left[\frac{1}{\tau_1^0} - \frac{1}{\tau_2^0} \right]^2} \hat{b}_{s-}^\dagger.$$

(6.11)

If we assign

$$(G_e)^{1/2} = \frac{\left[\frac{\omega}{Q_e} \right]^2 + \left[\frac{1}{\tau_1^0} - \frac{1}{\tau_2^0} \right]^2}{\left[\frac{\omega}{Q_e} \right]^2 - \left[\frac{1}{\tau_1^0} - \frac{1}{\tau_2^0} \right]^2},$$

(6.11) can be rewritten as

$$\hat{r}_{s+} = (G_e)^{1/2} \hat{b}_{s+} - (G_e - 1)^{1/2} \hat{b}_{s-}^\dagger.$$

(6.12)

Equation (6.12) is the universal relation between the input and output mode operators for a state squeezing.^{1,2} A cavity degenerate parametric amplifier is ideal for a state squeezing as long as the input signal bandwidth is much narrower than the amplifier bandwidth. This has already been indicated by Fig. 11 and by (6.7) and (6.8).

If we compare (5.7) and (5.8) for a highly excited pump-noise-suppressed laser with (6.1) and (6.2) for a cavity degenerate parametric amplifier, or equivalently (5.11) and (5.12) with (6.9) and (6.10), a certain analogy exists. If a pump-noise-suppressed laser has a zero internal loss and a cavity degenerate parametric amplifier is biased at the threshold [$1/\tau_1^0 = -1/\tau_2^0 = \frac{1}{2}(\omega/Q_e)$], the only difference is the dipole-moment fluctuation operators \tilde{G} and $\tilde{\Gamma}$ appearing in a pump-noise-suppressed laser equations. We will see in Sec. VIB that the dipole-moment fluctuation operator $\tilde{\Gamma}/2A_0 + \tilde{G}_1$ can be suppressed completely in the in-phase component, and that similar squeezing is obtained as a cavity degenerate parametric amplifier. We will also see that the dipole-moment fluctuation operator \tilde{G}_2 cannot be suppressed in the quadrature component, and therefore, that the minimum-uncertainty product (3.29) is never satisfied in a pump-noise-suppressed laser.

B. Internal field of a pump-noise-suppressed laser

The amplitude-noise $P_{\Delta\hat{A}}(\Omega)$ and phase-noise $P_{\Delta\hat{\phi}}(\Omega)$ spectra for the cavity internal field of a pump-noise-suppressed laser oscillator are calculated by (3.6) and (3.7) with $\langle |\tilde{\Gamma}_p(\Omega)|^2 \rangle = 0$. The characteristic examples of the amplitude-noise spectrum are shown in Fig. 12. Numerical parameters for Fig. 12 are the same as in Fig. 3 except that the internal loss is negligible as compared with the output coupling loss, i.e., $\omega/Q_0 \ll \omega/Q_e$. The amplitude-noise spectrum becomes Lorentzian when $R \gg 1$ in a similar way as does an ordinary laser [(3.14) or Fig. 3]. The spectral density is just one-half, however, that is,

$$P_{\Delta\hat{A}}(\Omega) = \frac{1}{2} \frac{\left[\frac{\omega}{Q} \right]}{\Omega^2 + \left[\frac{\omega}{Q} \right]^2}, \quad (6.13)$$

which is the same result as (6.4) for a cavity degenerate parametric amplifier. This means that the internal field features sub-Poissonian photon statistics having the variance $\langle \Delta\hat{n}^2 \rangle = 0.5\langle \hat{n} \rangle$.

The discussion in Sec. III indicates that the origin of the residual amplitude noise is the field zero-point fluctuation incident on the cavity. The gain saturation is not strong enough to suppress this noise source.

Characteristic examples of the phase noise spectrum are shown in Fig. 13. The same numerical parameters are used as Fig. 12. Since the phase-noise spectrum for $\alpha=0$ and $n_{sp}=1$ stems from the dipole noise operator \tilde{G}_i and the field zero-point fluctuation \hat{f}_i , the pump-fluctuation

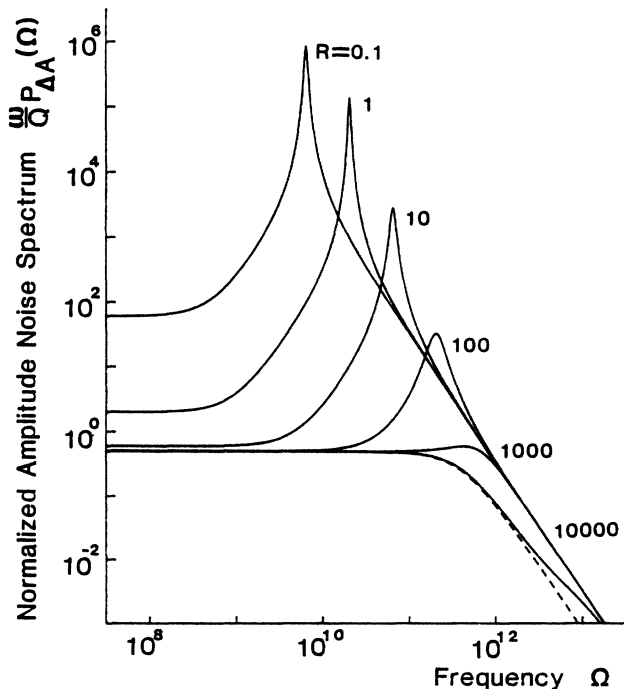


FIG. 12. Internal amplitude-noise spectra of a pump-noise-suppressed laser. $\omega/Q_0=0$.

suppression does not improve the ultimate phase-noise spectrum (3.17).

C. External field of a pump-noise-suppressed laser

The amplitude-noise $P_{\Delta\hat{r}}(\Omega)$ and phase-noise $P_{\Delta\hat{\psi}}(\Omega)$ spectra for the external output field of a pump-noise-suppressed laser oscillator are calculated using (3.19) and (3.20) with $\langle |\tilde{\Gamma}_p(\Omega)|^2 \rangle = 0$. Characteristic examples of the amplitude-noise spectrum are shown in Fig. 14(a). The same numerical parameters are used as in Fig. 12. The external amplitude-noise spectrum at $R \gg 1$ becomes lower than the standard quantum limit within the cavity bandwidth

$$P_{\Delta\hat{r}}(\Omega) = \frac{1}{2} \frac{\Omega^2}{\Omega^2 + \left[\frac{\omega}{Q} \right]^2}, \quad (6.14)$$

which is the same result as obtained in (6.7) for a cavity degenerate parametric amplifier. Although the amplitude-squeezing factor is only one-half for the internal field, the infinite amplitude squeezing is obtained for the external field in the low-frequency limit $\Omega \ll \omega/Q$. This is because the residual amplitude noise of the internal field destructively interferes with the reflected zero-point fluctuation to cancel each other out. The failure in suppressing the amplitude noise above the cavity bandwidth, $\Omega \geq \omega/Q$, stems from the absence of the amplitude

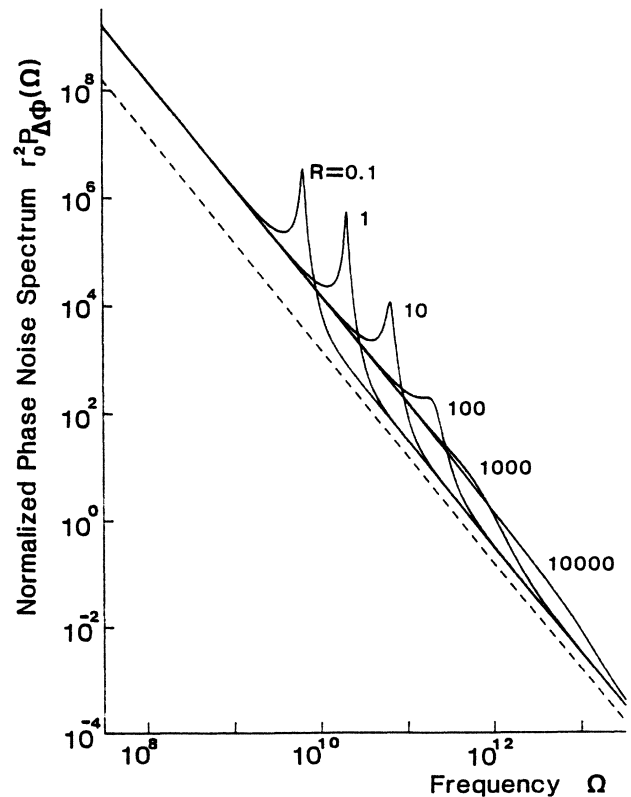
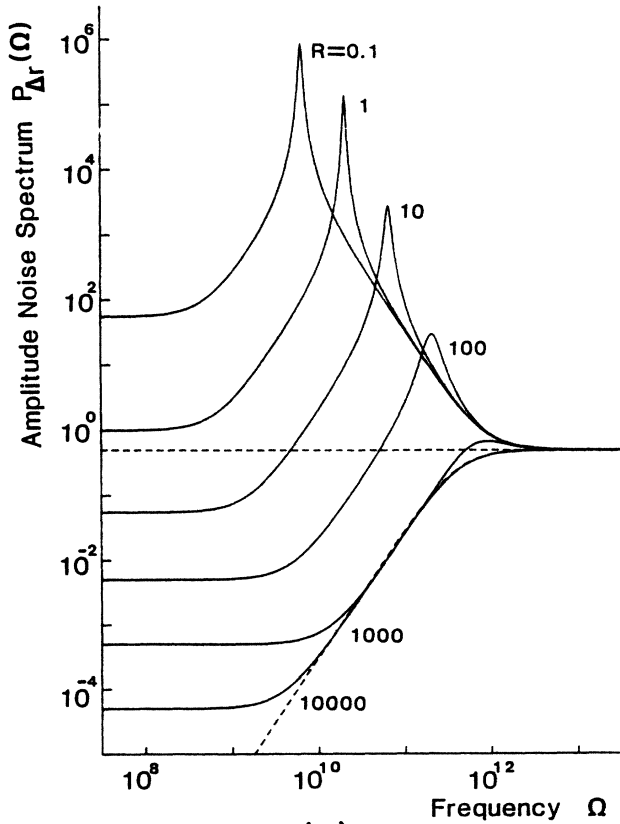


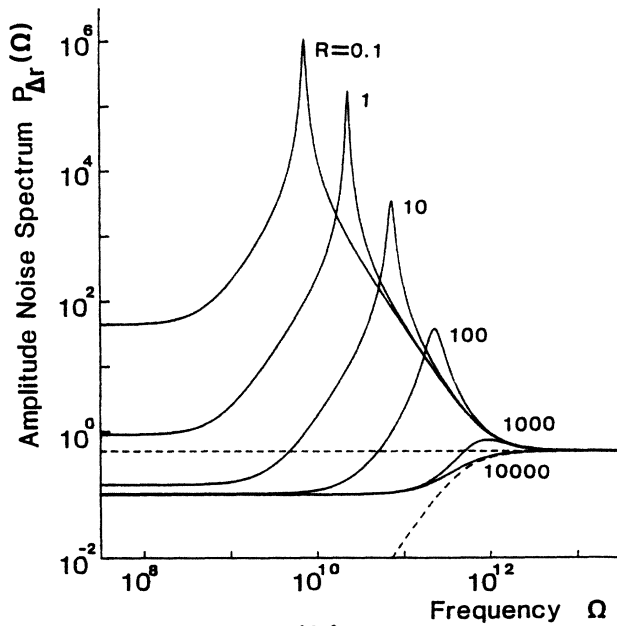
FIG. 13. Internal phase-noise spectra of a pump-noise-suppressed laser. $\omega/Q_0=0$.

noise in the internal field in this frequency region. The field zero-point fluctuation cannot enter into the cavity and is simply reflected back from the mirror.

Although the infinite amplitude squeezing can be obtained at $\Omega \ll \omega/Q$ when $\omega/Q_0 \ll \omega/Q_e$ as shown in Fig.



(a)



(b)

FIG. 14. External amplitude-noise spectra of a pump-noise-suppressed laser. (a) $\omega/Q_0=0$. (b) $\omega/Q_0=0.25(\omega/Q_e)$.

14(a), the squeezing factor is limited when the internal loss is not negligible, as shown in Fig. 14(b). This is because the quantum-mechanical correlation between the internal amplitude noise and the reflected zero-point fluctuation becomes imperfect due to the contribution of \hat{g}_r .

Figure 15 shows the external amplitude-noise spectrum $P_{\Delta r}(\Omega \cong 0)$ in the low-frequency region versus the normalized pumping level R as a function of the internal loss to output coupling loss ratio, Q_e/Q_0 . In order to obtain large amplitude squeezing, the value of ω/Q_e which is larger than ω/Q_0 and a higher pumping level are desirable.

Characteristic examples of the normalized phase-noise spectrum are shown in Fig. 16. It is clear that the ultimate phase-noise spectrum (3.23) is not altered by the pump-fluctuation suppression.

D. Uncertainty product

The product of the amplitude- and phase-noise spectra of a pump-noise-suppressed laser oscillator in the frequency region below the cavity bandwidth is

$$P_{\Delta r}(\Omega)P_{\Delta \hat{\psi}}(\Omega) = \frac{1}{2r_0^2}, \quad \Omega \leq \frac{\omega}{Q}. \quad (6.15)$$

This is twice as large as the minimum-uncertainty product (3.29). As shown in Sec. VIC the output field from a cavity degenerate parametric amplifier satisfies the minimum-uncertainty product (3.29) exactly. The obvious question is why a difference exists.

The difference stems from the fact that the quadrature

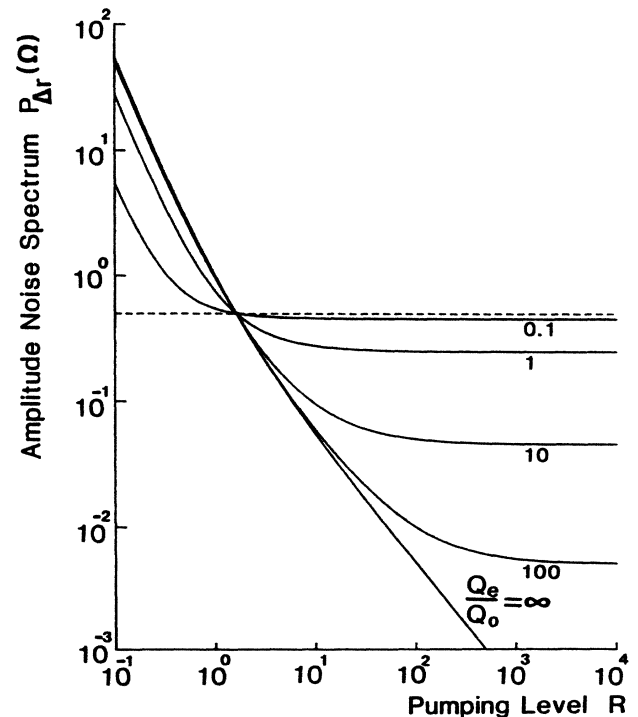


FIG. 15. External amplitude-noise spectral density $P_{\Delta r}(\Omega \cong 0)$ at low frequency vs pumping level R as a function of internal loss to output coupling loss ratio, Q_e/Q_0 .

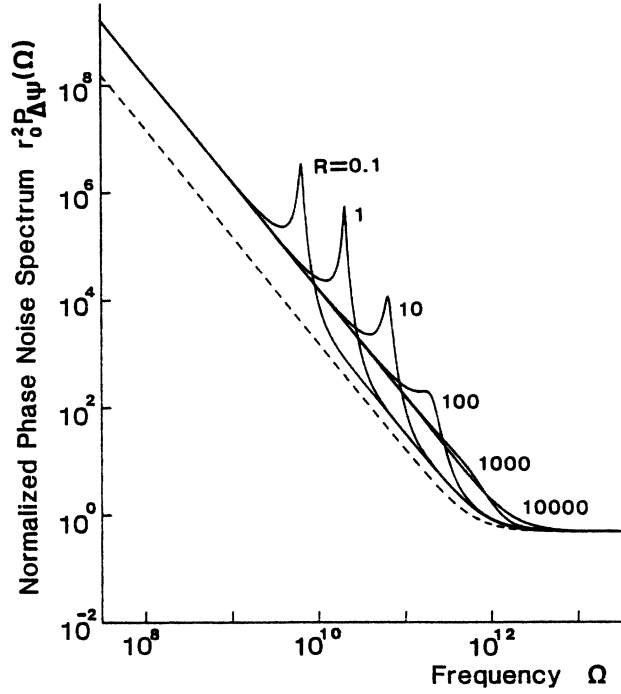


FIG. 16. External phase-noise spectra of a pump-noise-suppressed laser. $\omega/Q_0=0$.

component \tilde{G}_i of the dipole-moment noise operator is not suppressed by the gain saturation. While a cavity degenerate parametric amplifier and four-wave mixer⁵ have only one noise source, that is, the field zero-point fluctuation, a pump-noise-suppressed laser oscillator has two noise sources, the field zero-point fluctuation and the dipole-moment fluctuation.

The amplitude- and phase-noise spectra of an ideal pump-noise-suppressed laser are compared with the standard quantum limits of broadband coherent states in Figs. 17(a) and 17(b). If the “mode” is defined by the bandwidth much narrower than the laser cavity bandwidth, $B \ll \omega/Q$, the amplitude and phase noise of this laser output is close to the “amplitude squeezed state” shown in Fig. 1(b), even though it is not the “number-phase minimum uncertainty state.” If the mode is defined by the bandwidth much broader than the laser cavity bandwidth, $B \gg \omega/Q$, the amplitude and phase noise is close to the coherent state. One great advantage of using a semiconductor laser as an amplitude-squeezed-state generator is its broad bandwidth, i.e., the value of ω/Q is in the range of 10^{12} rad/sec.

VII. CONCLUSION

The principle conclusion of this paper is that an ideal laser oscillator preserves a nonclassical (sub-Poissonian) pump process, i.e., there is no hidden noise source in the conversion process from pumped electrons to emitted coherent photons. This can be clearly understood by the following consideration based on particle-number preservation.

If a laser-output coupling loss is much larger than its internal loss, $\omega/Q_e \gg \omega/Q_0$, and is pumped at well above

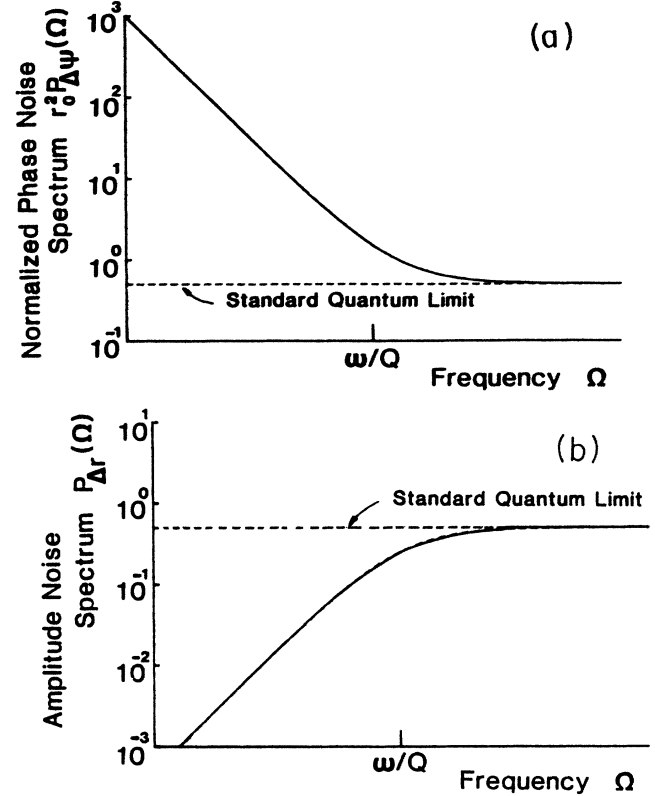


FIG. 17. (a) Normalized phase-noise spectrum $r_0^2 P_{\Delta\psi}(\Omega)$ and (b) amplitude-noise spectrum $P_{\Delta r}(\Omega)$ of a pump-noise-suppressed laser oscillator biased at well above threshold. r_0^2 is the average photon flux and ω/Q is the cavity bandwidth.

the threshold, $R \gg 1$, every pumped electron must sooner or later be emitted as an output coherent photon. The population-inversion decay rate $1/\tau_{st}$ due to stimulated emission completely dominates the decay rate $1/\tau_{sp}$ due to spontaneous emission and other nonradiative decay processes at a high pump level of $R \gg 1$. The internally emitted photons due to stimulated emission are extracted via an output coupling mirror before they are absorbed or scattered internally in a cavity satisfying $\omega/Q_e \gg \omega/Q_0$.

The slowest time constant for such an ideal laser is the photon lifetime $\tau_p = (\omega/Q)^{-1}$. If an emitted photon number is counted over a measurement time interval T_c , which is much longer than τ_p , the probability is negligible that any electrons or photons are left inside the laser. Therefore, the emitted photons should have the same sub-Poissonian statistics as the pumped electrons. Of course, if a measurement time interval is shorter than the photon lifetime, the emitted photons suffer from the random-output coupling process, with the sub-Poissonian behavior of the pumped electrons being consequently diluted by this randomness. Such behaviors of a pump-noise-suppressed laser are made very obvious in Fig. 17.

A high quantum efficiency is indeed only one criterion for such preservation of the pumped-electron statistics to the emitted-coherent-photon statistics. A semiconductor laser sometimes demonstrates an amazingly high quantum efficiency. It is also quite easy to regulate the electron-pumping process in an injection-current-driven semicon-

ductor laser by means of the so-called "high-impedance suppression."

ACKNOWLEDGMENT

The authors wish to thank Professor Hermann A. Haus of the Massachusetts Institute of Technology, Gunner Björk of the Royal Institute of Technology, and Fumio Kanaya and Nobuyuki Imoto for their useful discussions.

APPENDIX A: AMPLITUDE- AND PHASE-NOISE SPECTRA FOR INTERNAL FIELD

In this appendix (3.6) and (3.7) are derived using the quasilinearization (3.5a) and (3.5b) in the operator Langevin equations (2.1) and (2.10).

The linearized equations for the Hermitian amplitude, phase, and population-inversion fluctuating operators read

$$\frac{d}{dt} \Delta \hat{A} = \frac{1}{2A_0 \tau_{st}} \Delta \tilde{N}_c + \frac{1}{2} [(\tilde{G} + \hat{g} + \hat{f}) e^{j\Delta\hat{\phi}} + e^{-j\Delta\hat{\phi}} (\tilde{G}^\dagger + \hat{g}^\dagger + \hat{f}^\dagger)], \quad (\text{A1})$$

$$\frac{d}{dt} \Delta \hat{\phi} = \frac{\alpha}{2A_0^2 \tau_{st}} \Delta \tilde{N}_c + \frac{j}{2A_0} [(\tilde{G} + \hat{g} + \hat{f}) e^{j\Delta\hat{\phi}} - e^{-j\Delta\hat{\phi}} (\tilde{G}^\dagger + \hat{g}^\dagger + \hat{f}^\dagger)], \quad (\text{A2})$$

$$\frac{d}{dt} \Delta \tilde{N}_c = - \left[\frac{1}{\tau_{sp}} + \frac{1}{\tau_{st}} \right] \Delta \tilde{N}_c - 2 \frac{\omega}{Q} A_0 \Delta \hat{A} + \tilde{\Gamma}_p + \tilde{\Gamma}_{sp} + \tilde{\Gamma}. \quad (\text{A3})$$

The Fourier-series analysis with a period T that is made to approach infinity is used as the Fourier transform of (A1)–(A3). The power spectra of the operator $\hat{g}(t)$ is calculated by Wiener-Khintchin's theorem as

$$P_{\hat{g}}(\Omega) = \lim_{T \rightarrow \infty} \langle \hat{g}^\dagger(T, \Omega) \hat{g}(T, \Omega) \rangle, \quad (\text{A4})$$

and

$$\hat{g}(T, \Omega) = \sqrt{2/T} \int_{-T/2}^{T/2} \hat{g}(t) e^{j\Omega t} dt. \quad (\text{A5})$$

From (A1) to (A3) we can readily obtain the Fourier transforms $\Delta \hat{A}(\Omega)$ and $\Delta \hat{\phi}(\Omega)$ as

$$\Delta \hat{A}(\Omega) = \frac{-A_3 [\tilde{\Gamma}_p(\Omega) + \tilde{\Gamma}_{sp}(\Omega) + \tilde{\Gamma}(\Omega)] + (A_1 - j\Omega) H_r(\Omega)}{(A_2 A_3 + \Omega^2) + j\Omega A_1}, \quad (\text{A6})$$

and

$$\Delta \hat{\phi}(\Omega) = \frac{H_i(\Omega)}{\Omega A_0} + \frac{j A_2 A_4 H_r(\Omega) / \Omega - A_4 [\tilde{\Gamma}_p(\Omega) + \tilde{\Gamma}_{sp}(\Omega) + \tilde{\Gamma}(\Omega)]}{(A_2 A_3 + \Omega^2) + j\Omega A_1}. \quad (\text{A7})$$

Here the parameters A_1 – A_4 are given by (3.8)–(3.8d). $H_r(t)$ and $H_i(t)$ are defined by

$$H_r(t) = \frac{1}{2} [(\tilde{G} + \hat{g} + \hat{f}) e^{j\Delta\hat{\phi}} + e^{-j\Delta\hat{\phi}} (\tilde{G}^\dagger + \hat{g}^\dagger + \hat{f}^\dagger)], \quad (\text{A8})$$

and

$$H_i(t) = \frac{1}{2j} [(\tilde{G} + \hat{g} + \hat{f}) e^{j\Delta\hat{\phi}} - e^{-j\Delta\hat{\phi}} (\tilde{G}^\dagger + \hat{g}^\dagger + \hat{f}^\dagger)]. \quad (\text{A9})$$

The noise sources (A8) and (A9) have the multiplicative noise types. The correlation functions of $H_r(t)$ and $H_i(t)$, however, are not affected by the phase noise $\Delta\hat{\phi}$, because it is a slowly varying function as compared with the Markovian noise operators \tilde{G} , \hat{g} , and \hat{f} . That is, the noise sources $H_r(t)$ and $H_i(t)$ change and lose their memories completely before $\Delta\hat{\phi}$ changes appreciably.²¹ Therefore we obtain

$$\langle H_r(t) H_r(u) \rangle = \langle \tilde{G}_r(t) \tilde{G}_r(u) \rangle + \langle \hat{g}_r(t) \hat{g}_r(u) \rangle + \langle \hat{f}_r(t) \hat{f}_r(u) \rangle, \quad (\text{A10})$$

and

$$\langle H_i(t) H_i(u) \rangle = \langle \tilde{G}_i(t) \tilde{G}_i(u) \rangle + \langle \hat{g}_i(t) \hat{g}_i(u) \rangle + \langle \hat{f}_i(t) \hat{f}_i(u) \rangle. \quad (\text{A11})$$

Similarly, we obtain the cross-correlation function between $H_r(t)$ and $\tilde{\Gamma}(t)$ as

$$\langle H_r(t) \tilde{\Gamma}(u) \rangle = \langle \tilde{G}_r(t) \tilde{\Gamma}(u) \rangle. \quad (\text{A12})$$

Using (A10)–(A12) in (A6) and (A7), we then obtain (3.6) and (3.7).

APPENDIX B: AMPLITUDE- AND PHASE-NOISE SPECTRA FOR EXTERNAL FIELD

In this appendix (3.19) and (3.20) are derived from the relation (2.9). If we use the quasilinearizations (3.5a) for \hat{A} and (3.18) for \hat{r} together with (2.9), the Hermitian amplitude and phase-fluctuating operators are obtained as

$$\Delta \hat{r} = (\omega/Q_e)^{1/2} \Delta \hat{A} - \frac{1}{2(\omega/Q_e)^{1/2}} (\hat{f} e^{j\Delta\hat{\phi}} + e^{-j\Delta\hat{\phi}} \hat{f}^\dagger), \quad (\text{B1})$$

and

$$\Delta \hat{\psi} = \Delta \hat{\phi} + \frac{1}{2j r_0 (\omega/Q_e)^{1/2}} (\hat{f} e^{j\Delta\hat{\phi}} - e^{-j\Delta\hat{\phi}} \hat{f}^\dagger). \quad (\text{B2})$$

Using (A6) and (A7) in the Fourier analysis of (B1) and (B2) we obtain

$$\Delta \hat{r}(\Omega) = - \frac{\hat{f}_1(\Omega)}{(\omega/Q_e)^{1/2}} + \left[\frac{\omega}{Q_e} \right]^{1/2} \frac{-A_3 [\tilde{\Gamma}_p(\Omega) + \tilde{\Gamma}_{sp}(\Omega) + \tilde{\Gamma}(\Omega)] + (A_1 - j\Omega) H_r(\Omega)}{(A_2 A_3 + \Omega^2) + j\Omega A_1}, \quad (\text{B3})$$

and

$$\Delta\hat{\psi}(\Omega) = \frac{H_i(\Omega)}{\Omega A_0} + \frac{\hat{f}_2(\Omega)}{r_0(\omega/Q_e)^{1/2}} + \frac{jA_2A_4H_r(\Omega)/\Omega - A_4[\tilde{\Gamma}_p(\Omega) + \tilde{\Gamma}_{sp}(\Omega) + \tilde{\Gamma}(\Omega)]}{(A_2A_3 + \Omega^2) + j\Omega A_1}, \quad (\text{B4})$$

where $\hat{f}_1(\Omega)$ and $\hat{f}_2(\Omega)$ are the Fourier transforms of

$$\hat{f}_1(t) = \frac{1}{2}(\hat{f}e^{j\Delta\hat{\phi}} + e^{-j\Delta\hat{\phi}}\hat{f}^\dagger), \quad (\text{B5})$$

and

$$\hat{f}_2(t) = \frac{1}{2j}(\hat{f}e^{j\Delta\hat{\phi}} - e^{-j\Delta\hat{\phi}}\hat{f}^\dagger). \quad (\text{B6})$$

As was discussed in Appendix A, the slowly varying phase noise $\Delta\hat{\phi}$ does not affect the calculation of the correlation functions. From (B3) and (B4) we then obtain (3.19) and (3.20).

- ¹H. P. Yuen, *Phys. Rev. A* **13**, 2226 (1976).
²D. F. Walls, *Nature* **306**, 141 (1983).
³H. Takahashi, *Adv. Commun. Syst.* **1**, 227 (1965).
⁴H. P. Yuen and J. H. Shapiro, *Opt. Lett.* **4**, 334 (1979); R. Bondurant, P. Kumar, J. H. Shapiro, and M. Maeda, *Phys. Rev. A* **30**, 343 (1984).
⁵B. Yurke, *Phys. Rev. A* **32**, 300 (1985); R. E. Slusher, L. Hollberg, B. Yurke, J. C. Mertz, and J. F. Valley, *ibid.* **31**, 3512 (1985).
⁶M. D. Levenson, R. M. Shelby, M. Reid, and D. F. Walls, *Phys. Rev. A* **32**, 1550 (1985).
⁷R. E. Slusher, L. W. Hollberg, B. Yurke, J. C. Mertz, and J. F. Valley, *Phys. Rev. Lett.* **55**, 2409 (1985).
⁸Y. Yamamoto, O. Nilsson, and S. Saito, *Record of 3rd US-Japan Seminar on Coherence, Incoherence and Chaos in Quantum Electronics*, Nara, 1984 (unpublished), p. 70.
⁹Y. Yamamoto, N. Imoto, and S. Machida, *Phys. Rev. A* **33**, 3243 (1986).
¹⁰S. Machida and Y. Yamamoto, *Opt. Commun.* **57**, 290 (1986).
¹¹N. Imoto, H. A. Haus, and Y. Yamamoto, *Phys. Rev. A* **32**, 2287 (1985).
¹²H. A. Haus and Y. Yamamoto, *Phys. Rev. A* **34**, 270 (1986).
¹³B. E. A. Saleh and M. C. Teich, *Opt. Commun.* **52**, 429 (1985).
¹⁴E. Jakeman and J. G. Walker, *Opt. Commun.* **55**, 219 (1985).
¹⁵H. P. Yuen, *Proceedings of the 1975 Conference on Information Sciences and Systems*, Johns Hopkins University, 1975 (unpublished), p. 171.
¹⁶Y. Yamamoto and H. A. Haus, *Rev. Mod. Phys.* (to be published).
¹⁷H. P. Yuen, *Phys. Rev. Lett.* **56**, 2176 (1986).
¹⁸H. P. Yuen, *Phys. Lett.* **113A**, 405 (1986).
¹⁹Y. Yamamoto, S. Machida, and T. Yanagawa, *XIV International Quantum Electronics Conference, TuCC2*, San Francisco, 1986 (unpublished).
²⁰Y. Yamamoto, S. Machida, and O. Nilsson (unpublished).
²¹H. Haken, *Light and Matter*, Vol. XXV of *Handbuch der Physics* (Springer-Verlag, Berlin, 1970); *Light* (North-Holland, Amsterdam, 1981), Vols. 1 and 2.
²²M. Sargent III, M. O. Scully, and W. E. Lamb, Jr., *Laser Physics* (Addison-Wesley, Reading, Mass. 1974).
²³M. Lax and W. H. Louisell, *Phys. Rev.* **185**, 568 (1969).
²⁴Y. Yamamoto and N. Imoto, *J. Quantum Electron.* (to be published); O. Nilsson, Y. Yamamoto, and S. Machida, *ibid.* (to be published).
²⁵C. W. Gardinar and M. J. Collett, *Phys. Rev. A* **31**, 3761 (1985).
²⁶H. A. Haus and Y. Yamamoto, *Phys. Rev. A* **29**, 1261 (1984).
²⁷H. A. Haus and J. A. Mullen, *Phys. Rev.* **128**, 2407 (1962); C. M. Caves, *Phys. Rev. D* **26**, 1817 (1982).
²⁸P. Carruthers and M. M. Nieto, *Rev. Mod. Phys.* **40**, 411 (1968).
²⁹M. O. Scully and W. E. Lamb, Jr., *Phys. Rev.* **179**, 368 (1969).
³⁰H. A. Haus, *Proc. IEEE* **58**, 1599 (1970); W. H. Louisell, *Quantum Statistical Properties of Radiation* (Wiley, New York, 1973).
³¹A. W. Hull and N. H. Williams, *Phys. Rev.* **25**, 147 (1925); B. J. Thompson, D. O. North, and W. A. Harris, *RCA Rev.* **4**, 269 (1939).
³²J. Frank and G. Hertz, *Verh. Dtsch. Phys. Ges.* **16**, 457 (1914).
³³M. C. Teich and B. E. A. Saleh, *J. Opt. Soc. Am.* **2**, 275 (1985).
³⁴C. M. Caves and B. L. Schumaker, *Phys. Rev. A* **31**, 3068 (1985); B. L. Schumaker and C. M. Caves, *Phys. Rev. A* **31**, 3093 (1985).
³⁵G. Milburn and D. F. Walls, *Opt. Commun.* **39**, 401 (1981).